



# MARMARA UNIVERSITY
# FACULTY OF ENGINEERING

# DESIGN AND EXPERIMENTAL VALIDATION OF A SPRING-LOADED WET MULTI-DISC CLUTCH WITH HYDRAULIC DISENGAGEMENT FOR TRACTOR DROPBOX APPLICATIONS

MERTCAN TAŞCI

**GRADUATION PROJECT REPORT**
Department of Mechanical Engineering

**Supervisor**
Assist. Prof. Dr. SERKAN ÖĞÜT

ISTANBUL, 2026



# MARMARA UNIVERSITY
# FACULTY OF ENGINEERING

# DESIGN AND EXPERIMENTAL VALIDATION OF A SPRING-LOADED WET MULTI-DISC CLUTCH WITH HYDRAULIC DISENGAGEMENT FOR TRACTOR DROPBOX APPLICATIONS

MERTCAN TAŞCI (150421056)

**GRADUATION PROJECT REPORT**
Department of Mechanical Engineering

**Supervisor**
Assist. Prof. Dr. SERKAN ÖĞÜT

ISTANBUL, 2026

# MARMARA UNIVERSITY
## FACULTY OF ENGINEERING

Design and Experimental Validation of a Spring-Loaded

Wet Multi-Disc Clutch with Hydraulic Disengagement

for Tractor Dropbox Applications

by

Mertcan Taşcı

January 19, 2026, Istanbul

**SUBMITTED TO THE DEPARTMENT OF MECHANICAL ENGINEERING INPARTIAL FULFILLMENT OF THE REQUIREMENTS FOR THE DEGREE**

**OF**

**BACHELOR OF SCIENCE**

**AT**

**MARMARA UNIVERSITY**



Signature of Author .....  …..Mertcan Taşcı
Department of Mechanical Engineering

Certified By…… 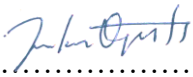 …….Assist. Prof. Dr. Serkan Öğüt
Project Supervisor, Department of Mechanical Engineering

Accepted By.....Prof. Dr. Bülent Ekici
Head of the Department of Mechanical Engineering

ISTANBUL, 2026

## ACKNOWLEDGEMENT

I would like to express my sincere gratitude to my advisor, Assist. Prof. Dr. Serkan Öğüt, for his valuable guidance, technical support, and continuous encouragement throughout this study. I also gratefully acknowledge TÜMOSAN Motor ve Traktör Sanayi A.Ş., and in particular the Transmission Technologies Department, for providing the technical infrastructure, test facilities, and system-level information required for this project. Their support was essential in enabling the analytical and experimental work presented in this thesis.

**January 2026** Mertcan Taşcı

# Contents

ACKNOWLEDGEMENT ..... i
ÖZET ..... iii
ABSTRACT ..... iv
SYMBOLS ..... v
ABBREVIATIONS ..... vi
1. INTRODUCTION ..... 1
2. METHOD ..... 3
2.1. Powertrain and Dropbox System Description ..... 3
2.2. Determination of Required Torque Based on Duty Cycle ..... 4
2.3. Wet Clutch Torque Capacity Calculation ..... 5
2.3.1. Selection of Design Torque from Duty Cycle Data ..... 8
2.3.2. Wet Clutch Torque Capacity and Required Axial Force ..... 9
2.4. Disc Spring (Belleville Spring) Modelling and Material Selection ..... 10
2.4.1. Geometric Definition and Disc Spring Groups ..... 10
2.4.2. Deflection Factors and Load-Deflection Formulation ..... 12
2.4.3. Design Stress ..... 14
2.4.4. Stacking of Disc Springs ..... 15
2.4.5. Iterative Spring Calculation Procedure and Operating Point Selection ..... 17
2.4.6. Calculations ..... 18
2.4.7. Material Selection and Heat Treatment ..... 22
2.5. Hydraulic Pressure Requirement for 4×2 Mode Switching ..... 23
2.6. Drag Torque Analysis ..... 24
3. RESULT & DISCUSSION ..... 28
3.1. Summary of Analytical Design Results ..... 28
3.2. Experimental Results ..... 31
3.3. Comparison of Analytical and Experimental Results ..... 33
4. CONCLUSION ..... 35
5. REFERENCES ..... 36

# ÖZET

**Traktör Dropbox Uygulamaları İçin Hidrolik Olarak Devre Dışı Bırakılan, Yay Ön Yüklemeli Islak Çok Diskli Kavramanın Tasarımı ve Deneysel Doğrulanması**

Bu çalışmada, tarım traktörlerinde dört tekerlekten çekiş (4×4) ve iki tekerlekten çekiş (4×2) modları arasında geçişi sağlayan bir dropbox sistemi için yay ön yüklemeli ve hidrolik olarak devre dışı bırakılan ıslak çok diskli kavrama sistemi tasarlanmış ve doğrulanmıştır. Tasarım sürecinde, traktörün gerçek çalışma koşullarını temsil eden görev çevrimi (duty cycle) verileri kullanılarak dropbox çıkışında oluşan maksimum tork gereksinimi belirlenmiştir.

Elde edilen tork gereksinimine bağlı olarak, ıslak kavrama sisteminin taşıması gereken eksenel kuvvet hesaplanmış ve bu kuvveti sağlayacak Belleville yay grubu BS EN 16983 ve BS EN 16984 standartları esas alınarak modellenmiştir. Yay geometrisi, malzeme seçimi ve ön yükleme miktarı belirlenirken gerilme sınırları ve montaj kısıtları dikkate alınmıştır. Hidrolik piston sistemi, yay ön yükünü aşarak kavramanın devreden çıkarılmasını sağlayacak şekilde boyutlandırılmıştır.

Ayrıca, kavramanın devre dışı olduğu durumda ortaya çıkan sürükleme torku (drag torque), yağ filmi kayma etkileri dikkate alınarak analitik olarak hesaplanmıştır. Analitik sonuçların doğrulanması amacıyla deneysel bir çalışma gerçekleştirilmiş ve kavramanın devreden çıkması için gerekli hidrolik basınç ölçülmüştür. Deneysel bulguların analitik hesaplamalarla uyumlu olduğu görülmüş ve geliştirilen tasarım yaklaşımının traktör dropbox uygulamaları için güvenilir ve uygulanabilir olduğu doğrulanmıştır.

# ABSTRACT

**Design and Experimental Validation of a Spring-Loaded Wet Multi-Disc Clutch with Hydraulic Disengagement for Tractor Dropbox Applications**

In this study, a spring-loaded wet multi-disc clutch system with hydraulic disengagement is designed and validated for a tractor dropbox application enabling transitions between four-wheel drive (4×4) and two-wheel drive (4×2) operating modes. Duty cycle data representing realistic tractor operating conditions were used to determine the maximum torque demand at the dropbox output.

Based on the calculated torque requirement, the required axial clamping force of the wet clutch was determined. A Belleville spring assembly capable of providing this preload was designed in accordance with BS EN 16983 and BS EN 16984 standards, considering geometric constraints, material properties, and stress limitations. A hydraulic piston system was dimensioned to overcome the spring preload and disengage the clutch during mode switching.

In addition, drag torque generated in the disengaged state due to viscous shear of the ATF was analytically evaluated. An experimental study was conducted to measure the hydraulic pressure required for clutch disengagement. The experimentally observed disengagement pressure showed good agreement with the analytically predicted value. The results confirm the validity of the proposed design methodology and demonstrate that the developed wet clutch system provides a reliable and effective solution for tractor dropbox applications.

## SYMBOLS

$F_p$: Single Belleville Spring Force
$T_a$: Torque transmitted by clutche
$n_f$: Number of friction surfaces
$T_f$: Total torque produced by clutches
$\mu$: Friction coefficient of the wet clutch material
$r_m$: Mean friction radius
$D_{o,f}, D_{i,f}$: Outer and inner diameter of the friction discs
$\omega_w$: Angular velocity of the wheel
$v_w$: Tractor speed
$r_w$: Wheel radius
$\omega_d$: Angular velocity of the output of dropbox
$i_{w,d}$: gear ratio between the wheel to the dropbox output shaft
$P_w$: Power at wheel
$N$: Number of Friction Discs
$\delta$: Diameter Ratio of Belleville Spring
$D_e$: Outer Diameter of Belleville Spring
$D_i$: İnner Diameter of Belleville Spring
$t$: Thickness of Belleville Spring
$h_0$: Initial cone hight of Belleville Spring without flat bearings
$l_0$: Free overall height of Belleville Spring in its initial position
$t'$: Reduced thickness of Belleville Spring
$K_1, K_2, K_3, K_4$: Constans of Belleville Spring
$E$: Elastic modulus of Belleville Spring
$v$: Poission ratio of Belleville Spring
$R_m$: Tensile strength of the Belleville Spring
$s$: Deflection of single Belleville Spring
$F_a$: Equivalent Belleville Spring Load
$n$: Number of single Belleville Springs stacked in parallel
$s_s$: Equivalent deflection of Belleville Springs
$i$: Number of Belleville Springs or packets stacked in series
$\sigma_I, \sigma_{II}, \sigma_{III}, \sigma_{IV}, \sigma_{OM}$: Design stresses at the points designated OM, I, II, III, IV
$L_0$: Length of spring stacked in series on in parallel, in the initial position
$A_p$: Effective piston area
$D_{o,p}, D_{i,p}$: Outer and Inner diameter of the piston
$F_h$: Piston force to bypass preload
$P$: Required piston pressure to bypass preload
$T_d$: Total drag torque
$T_{fa}$: The shear of ATF in the continuous section torque
$T_{ra}$: the shear of ATF in the ruptured section weighted by a “wetted fraction” torque
$T_{rm}$: The shear of the mist film in the ruptured section torque
$\mu_{atf}$: Dynamic viscosity of the ATF
$\Delta w$: Relative angular speed between the two friction disk sets
$h$: İnter-disk clearance of the friction discs
$r_{i,f}, r_{o,f}$: Inner and Outer radius of the friction disc

## ABBREVIATIONS

ATF: Automatic Transmission Fluid
BS: British Standard
DIN: Deutsches Institut für Normung
EN: European Norm
PTO: Power Take-Off

## List of Figures

Figure 1-1 Schematic of a Tractor Drivetrain ..... 1
Figure 1-2 Section View of Sample Dropbox ..... 2
Figure 2-1 Sample simplified sectional view of clutch assembly: a – blocking plate, b – hub, c – pressure plate, d – shaft, e – friction discs, f – separator discs..... 6
Figure 2-2 Mean friction radius of a friction disk ..... 7
Figure 2-3 Single Disc Spring (sectional view), including the relevant points of loading ..... 11
Figure 2-4 Sample Load/Deflection curve of single Belleville Spring ..... 13
Figure 2-5 Sample calculated stresses σ_OM versus deflection, with tensile strength R_mindicated ..... 15
Figure 2-6 Variations in load/deflection curves as a function of Belleville Spring stacking ... 16
Figure 2-7 The iterative spring–clutch matching procedure used to determine the operating deflection that satisfies both torque transmission and stress constraints ..... 18
Figure 2-8 Characteristics of Spring (Spring Load vs Travel Distance) ..... 20
Figure 2-9 Stress/Deflection Curve..... 23
Figure 2-10 Schematic of the film shape, yellow and green portions represent the ATF and the mist film, respectively ..... 25
Figure 3-1 Hydraulic pump and pressure measurement system used in the experimental study ..... 31
Figure 3-2 Dropbox assembly under test conditions..... 32
Figure 3-3 Pressure gauge reading at the onset of clutch engagement during pressure reduction ..... 33

## List of Tables

Table 2-1 Duty Cycle Result of a Tractor ..... 4
Table 2-2 Wheel radius and overall gear ratio used in the torque calculation ..... 8
Table 2-3 Calculated minimum required dropbox output torque values for the evaluated duty cycle load cases ..... 9
Table 2-4 Properties of the Friction Discs ..... 9
Table 2-5 Disc Spring Groups ..... 11
Table 2-6 Belleville Spring Physical Properties ..... 19
Table 2-7 Iterative calculation results ..... 21
Table 2-8 Geometrical Specifications for Piston ..... 24
Table 2-9 Results ..... 24
Table 2-10 Properties of ATF ..... 26
Table 2-11 Summarized table of drag torque ..... 27
Table 3-1 Belleville Spring Properties ..... 29
Table 3-2 Friction Disc Properties ..... 29
Table 3-3 Values from Duty Cycle ..... 29
Table 3-4 Dropbox Torque and Spring Force ..... 30
Table 3-5 Piston Pressure (To Bypass Preload) ..... 30
Table 3-6 Drag Torque ..... 30

# 1. INTRODUCTION

Modern agricultural tractors operate under a wide range of working conditions, including heavy-duty field operations and light-duty road transport. In order to satisfy these different operating requirements, tractors are commonly equipped with selectable drivetrain configurations such as two-wheel drive (4×2) and four-wheel drive (4×4). The ability to reliably engage and disengage the front axle is essential for providing sufficient traction while maintaining efficiency, durability, and fuel economy [1].

In a typical tractor powertrain, mechanical power is transmitted from the engine through the gearbox and transmission housing to the rear axle, Power Take-Off (PTO), and auxiliary drivetrain components as can be seen in **Hata! Başvuru kaynağı bulunamadı.**. One of the key components in this system is the dropbox, which enables torque transfer from the main drivetrain to the front axle. By controlling this torque path, the dropbox allows the tractor to operate in either 4×2 or 4×4 mode depending on operating conditions [1].

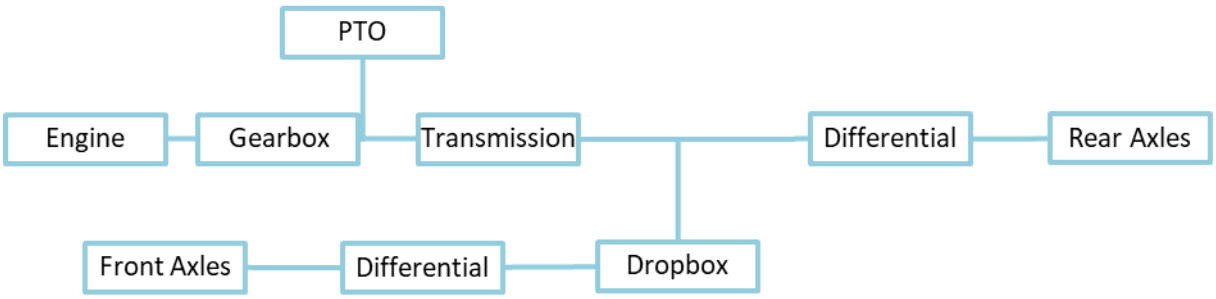


Figure 1-1 Schematic of a Tractor Drivetrain

During demanding field operations such as flowing or operation on soft terrain, engaging the front axle improves traction and vehicle stability. However, during road transport or light-duty operation, disengaging the front axle reduces power losses, mechanical wear, and unnecessary loading of drivetrain components. Therefore, the dropbox system must satisfy two conflicting requirements: it must safely transmit high torque levels during 4×4 operation, while also ensuring reliable disengagement with minimal residual torque during 4×2 operation.

The dropbox system investigated in this study utilizes a wet multi-disc clutch actuated by preloaded Belleville (disc) springs as seen in **Hata! Başvuru kaynağı bulunamadı.**. In the engaged state, the preload force generated by the disc springs applies a normal force on the friction discs, enabling torque transmission to the front axle shaft. Belleville springs were specifically selected for this application due to their ability to generate high clamping forces within a limited axial installation space, which is a critical constraint in the dropbox design [2, 8]. Compared to conventional helical springs, they offer a superior force-to-space ratio suitable for compact heavy-duty clutches. When switching from 4×4 to 4×2 mode, hydraulic pressure is applied to overcome the spring preload, thereby eliminating the contact force between the friction discs and interrupting torque transmission.

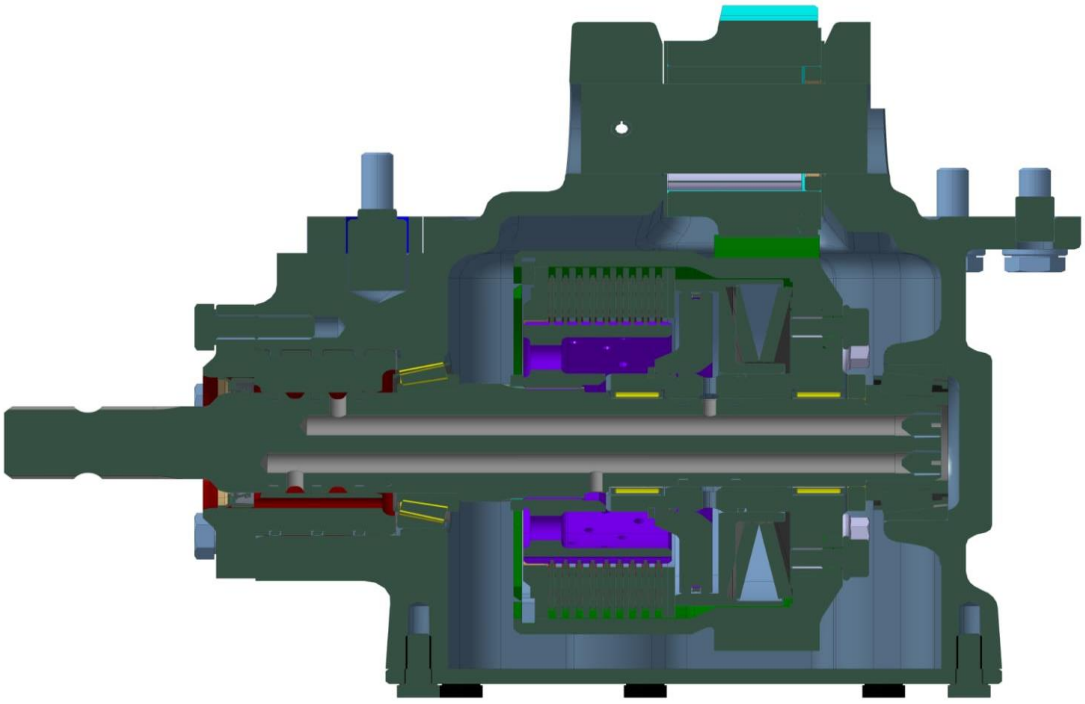

Figure 1-2 Section View of Sample Dropbox

Designing such a system requires a systematic evaluation of drivetrain loads under realistic operating conditions. In tractor design practice, duty cycles are commonly used to represent the range of loads encountered during the service life of the vehicle. These duty cycles provide a reliable basis for determining torque requirements at different drivetrain components, including the front axle and the dropbox [1]. In this study, duty cycle data corresponding to the tractor with the highest torque capacity were selected to adopt a conservative, worst-case design approach.

Based on the required torque at the front wheels, the torque demand at the dropbox output was determined through reverse drivetrain analysis. This torque requirement was used to define the minimum torque capacity of the wet clutch system. The required normal force acting on the friction discs was calculated accordingly, and the preload force of the Belleville springs was determined using standardized calculation methods [2,3]. Spring geometry and material selection were carried out in accordance with relevant standards and manufacturer data [2–5].

In addition to torque transmission capability, the disengaged behaviour of the clutch system was also evaluated. When the wet clutch is disengaged, viscous shear of the lubricant film between the friction discs results in a residual drag torque. Although this drag torque is significantly smaller than the transmitted torque during engagement, it may still influence vehicle behaviour during 4×2 operation. Therefore, the drag torque was evaluated using established analytical and experimental models reported in the literature [6,7,9].

Finally, experimental tests were conducted to validate the analytical design. The hydraulic pressure required to overcome the spring preload and disengage the clutch was measured and compared with theoretical predictions. The close agreement between experimental and analytical results confirms the validity of the adopted design methodology and supports the applicability of the proposed approach for tractor dropbox systems.

# 2. METHOD

This chapter outlines the comprehensive design and verification methodology employed for the spring-loaded wet multi-disc clutch system. The design process begins with a detailed description of the tractor powertrain architecture and the specific functional requirements of the dropbox unit. To ensure a realistic sizing approach, the torque demand at the dropbox output is derived from field duty cycle data rather than nominal engine characteristics. Based on these inputs, the wet clutch torque capacity is calculated, and the required axial clamping force is determined. A significant portion of the methodology focuses on the analytical modelling of the Belleville spring assembly according to BS EN 16983 and BS EN 16984 standards, covering geometric dimensioning, stress analysis, and stacking configuration. Finally, the hydraulic pressure required for clutch disengagement and the residual drag torque generated in the open clutch state are evaluated analytically to verify the system's operational limits.

## 2.1. Powertrain and Dropbox System Description

The powertrain of an agricultural tractor is designed to transmit engine power to multiple outputs, including the rear axle, front axle, and PTO, while enabling flexible operation under varying load and driving conditions. In the investigated tractor configuration, mechanical power is generated by the engine and transmitted through the gearbox and transmission housing before being distributed to the drivetrain components [1].

As shown in the simplified powertrain layout presented in Figure 1-1 Schematic of a Tractor Drivetrain, the gearbox provides the required forward and reverse gear ratios and allows adjustment of the traction level according to operating conditions. In addition to the main gearbox, the transmission housing incorporates an additional gear group consisting of high, medium, and low ranges. This range selection enables further adaptation of vehicle speed and torque to field or transport operations [1].

The transmission housing distributes power to the permanently driven rear axle, the PTO shaft, and the dropbox unit. The rear axle remains continuously engaged, whereas the front axle is selectively driven through the dropbox system depending on the selected operating mode.

The dropbox is mechanically mounted beneath the transmission housing and serves as the interface between the main drivetrain and the front axle system. Its primary function is to control the transfer of torque to the front axle, thereby enabling operation in either two-wheel drive (4×2) or four-wheel drive (4×4) mode. Torque is transmitted from the dropbox to the front differential through appropriate drive shafts.

In the studied system, front axle engagement is controlled by a wet multi-disc clutch integrated within the dropbox. The clutch pack consists of alternating friction and separator discs operating in an oil bath. Torque transmission is achieved when sufficient normal force is applied to the clutch pack, allowing frictional contact between the discs.

The normal force required for torque transmission is provided by Belleville (disc) springs assembled in a preloaded configuration. Belleville springs were selected due to their ability to generate high force levels within a limited installation space, which is a critical constraint in the dropbox design. In the default state, the spring preload applies a compressive force on the clutch pack, enabling torque transmission from the dropbox input gear to the output shaft connected to the front axle. This condition corresponds to four-wheel drive (4×4) operation.

The selection of Belleville springs and their advantages compared to other spring types are discussed in detail in the following sections [2,3,8].

Transition from four-wheel drive (4×4) to two-wheel drive (4×2) is achieved by hydraulic disengagement of the clutch system. When hydraulic pressure is applied to the piston integrated into the dropbox, the preload force of the Belleville springs is counteracted. As a result, the contact force between the friction discs is removed, and torque transmission to the front axle is interrupted. In this disengaged state, the front axle rotates freely without receiving driving torque from the engine.

The combined use of spring-loaded engagement and hydraulically controlled disengagement allows the dropbox system to meet two essential requirements: reliable torque transmission under high-load operating conditions and efficient decoupling of the front axle during low-load or transport operation. This system configuration forms the basis for the analytical calculations and experimental investigations presented in the subsequent sections.

### 2.2. Determination of Required Torque Based on Duty Cycle

In agricultural tractor design, drivetrain components must be sized based on realistic operating conditions rather than nominal engine output alone. For this purpose, duty cycle data are commonly used to represent the distribution of loads, speeds, and operating durations encountered during real service conditions. Duty cycles provide a systematic basis for identifying critical load cases and defining conservative design inputs for drivetrain components [1].

In this study, duty cycle results (DC results) generated from a validated tractor simulation model were used as the primary input for torque determination. In this study, duty cycle results (DC results) were generated using a comprehensive tractor simulation model developed in Romax software by the company's simulation department. The model's architecture and load distribution logic are based on the tractive performance methodologies outlined by Renius [1], and the outputs were validated against field data. The simulation outputs include engine speed, engine torque, tractor speed, and the distribution of power to different drivetrain outputs such as the rear axle, front axle, and PTO. An excerpt of the duty cycle output data used in this study is presented in **Hata! Başvuru kaynağı bulunamadı.**.

| 3. ADIM | 2. adımda elde edilen verimlerle oluşturulan csv output dosyası ile, generated from center bins metodu ile condense edilen DC'den Power out 4wd hesaplanır. Traktör hızı 13 km/h'in altındaysa 0.35 oranında ön aksa güç verilir; üstündeyse tamamı arka ak | | | | | | | | | | | | | | | | | | |
|---|---|---|---|---|---|---|---|---|---|---|---|---|---|---|---|---|---|---|---|
| | | | Power Input | ----- | ----- | Power Out 4wd | ----- | ----- | Power Out left | ----- | ----- | Power Output PTO | ----- | ----- | Power Out right | ----- | ----- | | |
| Name | Duration | Tempera | Speed (rpm) | Torque (I | Power (kW) | Speed (rpm) | Torque (I | Power (k | Speed (rpm) | Torque (I | Power (k | Speed (rpm) | Torque (Ni | Power (k | Speed (rpm) | Torque (Ni | Power (kW | Power Out 4wd | Tractor speed |
| F01 Load case 1 | 12,9571 | 85 | 2300 | 74,9798 | 18,05929 | -61 | 2226 | -14,3 | 4 | | 0 | | | | 4 | | 0 | -4,99942485 | 1,07 |
| F02 Load case 1 | 10,6203 | 85 | 2300 | 90,848 | 21,88124 | -75 | 2228 | -17,4 | 4 | | 0 | | | | 4 | | 0 | -6,0929841 | 1,30 |
| F03 Load case 1 | 10,6203 | 85 | 2300 | 110,425 | 26,59634 | -96 | 2192 | -22 | 6 | | 0 | | | | 6 | | 0 | -7,7134302 | 1,68 |

Table 2-1 Duty Cycle Result of a Tractor

Due to corporate confidentiality policies, only a representative excerpt of the dataset is presented.

According to the duty cycle definition applied in the simulation model, the distribution of driving power between the front and rear axles depends on tractor speed. When the tractor speed is below 13 km/h, a portion of the engine power is transferred to the front axle during four-wheel drive operation. At higher vehicle speeds, front axle engagement is typically avoided in order to reduce drivetrain wind-up, mechanical losses, and unnecessary loading of front axle components. This operating strategy is consistent with common tractor drivetrain design

practices, where four-wheel drive is primarily intended for low-speed, high-traction conditions [1].

From the duty cycle output, the power delivered to the front axle during four-wheel drive operation was extracted for all relevant load cases. These values represent the power that must be transmitted through the dropbox under realistic operating conditions. In order to ensure a safe and conservative design, the tractor configuration with the highest torque capacity was selected, and the maximum front axle power observed in the duty cycle data was taken as the critical design input.

The required torque at the dropbox output was determined through reverse drivetrain analysis based on the extracted front axle power values. This approach allows the torque demand at the dropbox to be derived directly from the operating conditions at the front wheels without relying on isolated peak engine values. The resulting torque values define the minimum torque capacity that the wet clutch system integrated into the dropbox must safely transmit without slip.

By basing the torque requirement on duty cycle data rather than single operating points, the design process accounts for both load magnitude and operating duration. This methodology ensures that the dropbox system is sized to withstand the most severe and representative operating conditions expected during the tractor's service life. The torque values obtained in this section form the basis for the wet clutch torque capacity calculations presented in the following section.

### 2.3. Wet Clutch Torque Capacity Calculation

The torque requirement obtained from the duty cycle analysis represents the minimum torque that must be transmitted by the dropbox during four-wheel drive operation. In the investigated system, torque transmission to the front axle is achieved by a wet multi-disc clutch integrated into the dropbox. Therefore, the clutch must be designed to provide sufficient torque capacity to transmit the required torque without slip under the most severe operating conditions.

Wet multi-disc clutches transmit torque through frictional interaction between alternating friction and separator discs that are axially clamped by an external force. By increasing the number of friction interfaces, higher torque levels can be transmitted within a compact axial space, which makes this clutch type suitable for tractor and heavy-duty drivetrain applications [8,9].

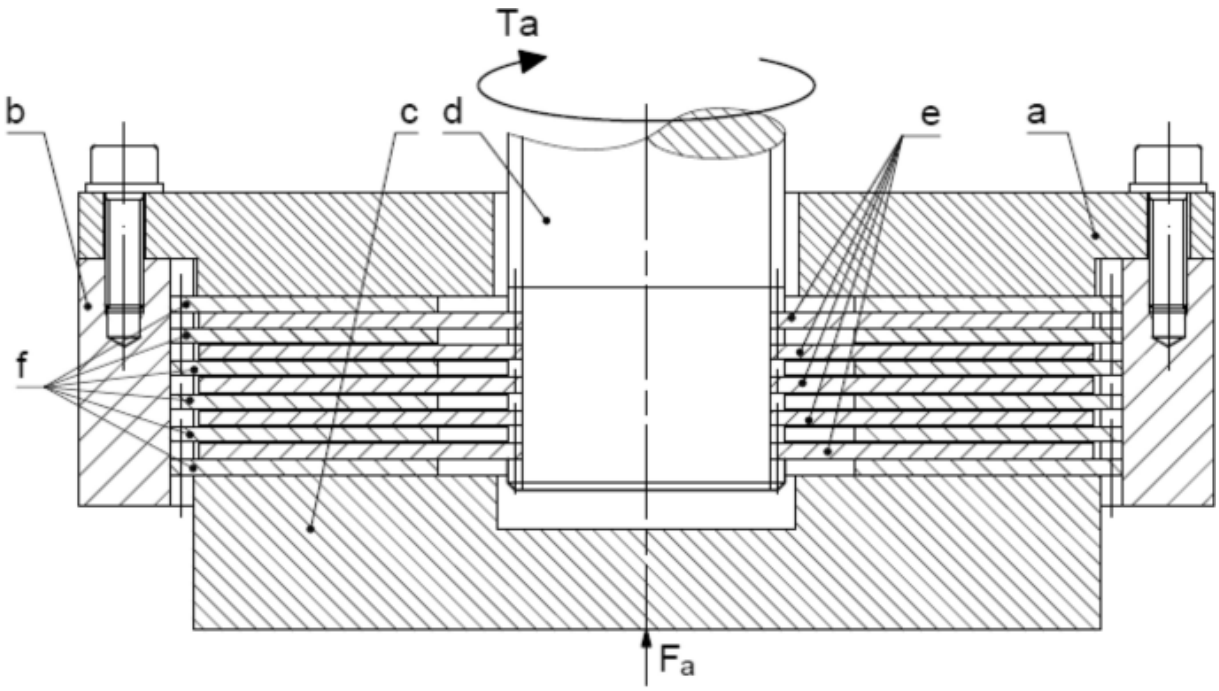


Figure 2-1 Sample simplified sectional view of clutch assembly: a – blocking plate, b – hub, c – pressure plate, d – shaft, e – friction discs, f – separator discs

As seen in Figure 2-1, the simplified sectional view of the clutch assembly illustrates the key components involved in torque generation. The mechanism consists of alternating friction discs (e) and separator discs (f) housed within the hub (b) and constrained by the blocking plate (a). The pressure plate (c) applies an axial force ($F_a$) to the disc stack, creating the necessary frictional contact to transmit torque ($T_a$) to the shaft (d).

In the fully engaged condition, all friction and separator discs rotate at the same angular velocity. Under this condition, viscous shear effects of the lubricant do not contribute to torque transmission, and the transmissible torque can be described using a friction-based model [6]. Accordingly, the total torque transmitted by a multi-disc wet clutch can be expressed as the sum of the torque contributions of the individual friction interfaces:

$$T_a = n_f \times T_t \tag{2.3.1}$$

Where $T_a$ is the torque transmitted by clutches, $n_f$ is the number of friction surfaces, and $T_t$ represents the torque transmitted by a single friction interface.

The torque transmitted by a single friction interface can be written as:

$$T_t = \mu \times r_m \times F_a \tag{2.3.2}$$

Where $\mu$ is the friction coefficient of the wet clutch material, $r_m$is the mean friction radius, and $F_a$ is the equivalent Belleville Spring load.

The mean friction radius is determined based on the inner and outer radius of the friction surfaces and is calculated as:

$$r_m = \frac{2}{6} \times \frac{D_o^3 - D_i^3}{D_o^2 - D_i^2} \tag{2.3.3}$$

Where $D_o$ and $D_i$ represent the outer and inner diameters of the friction discs, respectively.

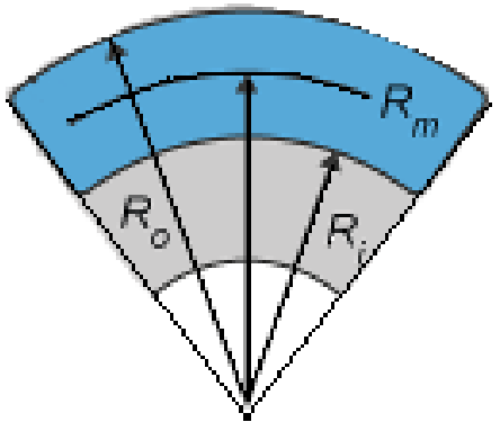


Figure 2-2 Mean friction radius of a friction disk

The mean friction radius represents the (as seen in Figure 2-2) effective radius at which the friction forces act to transmit torque in the clutch. Since the friction force is distributed over the annular contact area between the inner and outer radii of the friction surfaces, the transmitted torque cannot be accurately represented by using either the inner radius or the outer radius alone. Instead, an equivalent radius is defined to account for the contribution of friction forces across the entire contact area.

The mean friction radius is derived by integrating the frictional moment over the contact surface and assuming a uniform pressure distribution. This approach provides a realistic representation of torque transmission in multi-disc wet clutches and is widely adopted in clutch design literature [8,9].

By combining the above expressions, the minimum axial force required to transmit the target torque can be obtained as:

$$F_a = \frac{T_a}{\mu \times r_m} \tag{2.3.4}$$

In this study, the required clutch torque was set equal to the maximum torque demand determined from the duty cycle-based analysis described in Section 2.2. The number of friction interfaces and clutch geometry were defined based on the existing system configuration, while the friction coefficient was selected in accordance with values reported for wet clutch applications in the taken from manufacturer data.

The calculated axial force represents the total compressive force that must be applied to the clutch pack during four-wheel drive operation. In the investigated dropbox system, this force is generated by preloaded Belleville springs. The selection of the spring type and the preload calculation are presented in the following section.

It should be noted that wet multi-disc clutches experience drag torque in the disengaged condition due to oil shear between rotating discs. However, drag torque does not contribute to torque transmission capacity in the engaged state and is therefore excluded from the torque capacity calculation. Drag torque effects are evaluated separately in Section 2.6 using established analytical and experimental models [6,7].

### 2.3.1. Selection of Design Torque from Duty Cycle Data

The selection of the design torque for wet clutch sizing was based on the duty cycle data introduced in Section 2.2. For each relevant duty cycle load case, the power delivered to the front wheels during four-wheel drive operation was used as the primary input for the torque calculation.

The wheel radius used in the analysis was taken from the vehicle data of the investigated tractor, and the overall gear ratio between the wheel and the dropbox output shaft was calculated based on the drivetrain configuration. These parameters were used directly in the torque calculation without explicitly evaluating intermediate rotational speeds of individual drivetrain components.

The angular velocity of the wheel was expressed as:

$$\omega_w = \frac{v_w}{r_w} \tag{2.3.1.1}$$

Where $\omega_w$ is the angular velocity of the wheel, $v_w$ is the tractor speed, and $r_w$ is the wheel radius.

By incorporating the overall gear ratio between the wheel and the dropbox output shaft, the angular velocity at the dropbox output shaft can be written as:

$$\omega_d = i \times \omega_w \tag{2.3.1.2}$$

Where $\omega_d$ is the angular velocity of the output of dropbox, and $i$ represents the gear ratio between the wheel to the dropbox output shaft.

Using the fundamental relationship between power, torque, and angular velocity, the minimum required torque at the dropbox output shaft was calculated as:

$$T_a = \frac{P_w}{w_d} \tag{2.3.1.3}$$

Where $P_w$ represents the power at wheel.

Substituting the above expressions, the required dropbox output torque can be written directly as:

$$T_a = \frac{P_w \times r_w}{i \times \omega_w} \tag{2.3.1.4}$$

This calculation was applied to all duty cycle cases for which front axle power transmission is active. The wheel radius and the calculated overall gear ratio used in the analysis are summarized in Table 2-2, while the resulting minimum required dropbox output torque values for each load case are presented in Table 2-3.

Table 2-2 Wheel radius and overall gear ratio used in the torque calculation

| | |
|---|---|
| Wheel Radius (m) | 0,619 |
| Gear Ratio (From Wheel to Dropbox output shaft) | 13,6 |

Table 2-3 Calculated minimum required dropbox output torque values for the evaluated duty cycle load cases

| Power at Wheel (kW) | Tractor Speed (km/h) | Min. Dropbox Output Torque (Nm) |
|---|---|---|
| 4,99 | 1,07 | 767,2 |
| 6,09 | 1,3 | 767,6 |
| 7,71 | 1,68 | 752,0 |

Among the evaluated load cases, the maximum required dropbox output torque was obtained for a front wheel power of 6.09 kW at a tractor speed of 1.3 km/h. For this operating condition, the calculated minimum dropbox output torque was 767.64 Nm, which represents the highest torque demand observed within the duty cycle data set. This torque value was therefore selected as the design torque input for wet clutch sizing and was used consistently in all subsequent clutch capacity and spring preload calculations.

### 2.3.2. Wet Clutch Torque Capacity and Required Axial Force

In order to transmit the design torque selected in Section 2.3.1, the wet clutch assembly inside the dropbox must generate a sufficient torque capacity through friction. This torque capacity is provided by the normal (axial) force applied to the clutch pack and the friction characteristics of the clutch discs.

The wet clutch system considered in this study consists of multiple friction discs operating in an oil-lubricated environment. The geometric properties of the friction discs, the number of discs, the number of friction interfaces, and the friction coefficient were obtained from the clutch disc manufacturer. These parameters correspond to an existing and currently used clutch disc design. The relevant clutch disc data used in the analysis are summarized in Table 2-4.

Table 2-4 Properties of the Friction Discs

| | | |
|---|---|---|
| $N$ | 9 | |
| $n_f$ | 18 | |
| $D_{o,f}$ | 133,35 | mm |
| $D_{i,f}$ | 100 | mm |
| $\mu$ | 0,14 | |
| $r_m$ | 58,73 | mm |

The design torque $T_A$ used in the calculation corresponds to the maximum required dropbox output torque identified in Section 2.3.1 and was determined as 767.64 Nm based on the duty cycle data. The number of friction interfaces $n_f$ was defined according to the total number of friction discs used in the clutch pack, while the friction coefficient $\mu$ was taken directly from the manufacturer-provided data for the selected wet clutch friction material. The mean friction radius $r_m$ was calculated using the inner and outer diameters of the friction discs given in Table 2-4

By substituting these parameters into the torque–axial force relationship defined in Equation (2.3.4), the minimum axial force required to transmit the selected design torque without slip

was calculated. The resulting required axial force acting on the clutch pack was found to be 1296,6 N.
This axial force represents the minimum force that must be provided by the Belleville spring stack under preload conditions to ensure reliable torque transmission during four-wheel drive operation. The calculated axial force value was subsequently used as the primary input for the disc spring selection and preload analysis presented in the following section.

### 2.4. Disc Spring (Belleville Spring) Modelling and Material Selection

Disc springs, also known as Belleville springs, are widely used in compact drivetrain and clutch applications due to their ability to generate high axial forces within limited installation space. In the studied dropbox wet clutch system, disc springs are employed to provide the required axial preload acting on the friction disc pack, which directly determines the torque transmission capability of the clutch.
The design of the disc spring system must simultaneously satisfy multiple requirements. First, the spring assembly must generate sufficient axial force to transmit the required clutch torque under the most demanding operating condition obtained from the duty cycle analysis. Second, the spring must operate within acceptable stress limits to ensure structural integrity and durability. Finally, the spring configuration must be compatible with the geometric constraints of the dropbox housing and the practical limitations of manufacturing and assembly.
To address these requirements, the disc spring modelling procedure in this study follows a structured approach based on applicable international standards. The geometric definitions and classification of disc springs are taken from BS EN 16983:2016 (British Standard European Norm), which specifies the relevant dimensional parameters, geometric groups, and general manufacturing guidelines for disc springs [2]. The analytical formulation for load–deflection behaviour, stress evaluation at critical locations, and stacking effects is based on BS EN 16984:2016 [3].
In addition to mechanical modelling, material selection plays a critical role in disc spring performance. BS EN 16983:2016 provides guidance on suitable material standards for disc springs depending on their geometric classification and application conditions. Based on this guidance, candidate spring steels were evaluated using EN 10132-4, which defines mechanical property and hardness requirements for cold rolled strip steels intended for heat treatment [4]. The compatibility of the selected material with appropriate heat treatment conditions was further verified using DIN 17221 (Deutsches Institut für Normung), which specifies heat treatment practices for spring steels [5].
All disc spring calculations in this study were carried out using an iterative numerical approach implemented in a spreadsheet environment. This method allows the continuous evaluation of spring force, stress levels, and clutch torque capacity as a function of spring deflection, ensuring a consistent link between disc spring behaviour and wet clutch performance. The detailed modelling steps, including geometric classification, analytical formulations, stacking methodology, and material verification, are presented in the following subsections.

#### 2.4.1. Geometric Definition and Disc Spring Groups

The geometric definition and classification of disc springs used in this study are based on BS EN 16983:2016, which provides standardized dimensional parameters, group classifications,

and general manufacturing guidelines for disc springs [2]. According to the standard, a disc spring is characterized by its conical geometry and is described using a limited set of fundamental dimensions that govern its mechanical behaviour under axial loading.

The primary geometric parameters of a disc spring include the outer diameter $D_e$, inner diameter $D_i$, thickness $t$, reduced thickness $t'$(where applicable), free height $l_0$, and free cone height $h_0$. These parameters directly influence the stiffness characteristics, load capacity, and allowable deflection range of the spring, and they form the basis of all subsequent load–deflection and stress calculations presented in this study.

BS EN 16983:2016 classifies disc springs into three geometric groups according to the presence of flat bearing surfaces and the ratio between the reduced thickness and the nominal thickness. This classification is summarized in Table 2-5, where Group 1 and Group 2 correspond to disc springs without flat bearing surfaces, while Group 3 represents disc springs with flat bearing surfaces. The reduced thickness ratio $t'$serves as the primary distinguishing parameter between these groups and defines the applicable geometric range for each classification.

Table 2-5 Disc Spring Groups

| Group | $t$ (mm) | With flat bearings and reduced thickness |
|---|---|---|
| 1 | $< 1{,}25$ | No |
| 2 | $1{,}25 < t < 6$ | No |
| 3 | $6 < t \leq 14$ | Yes |

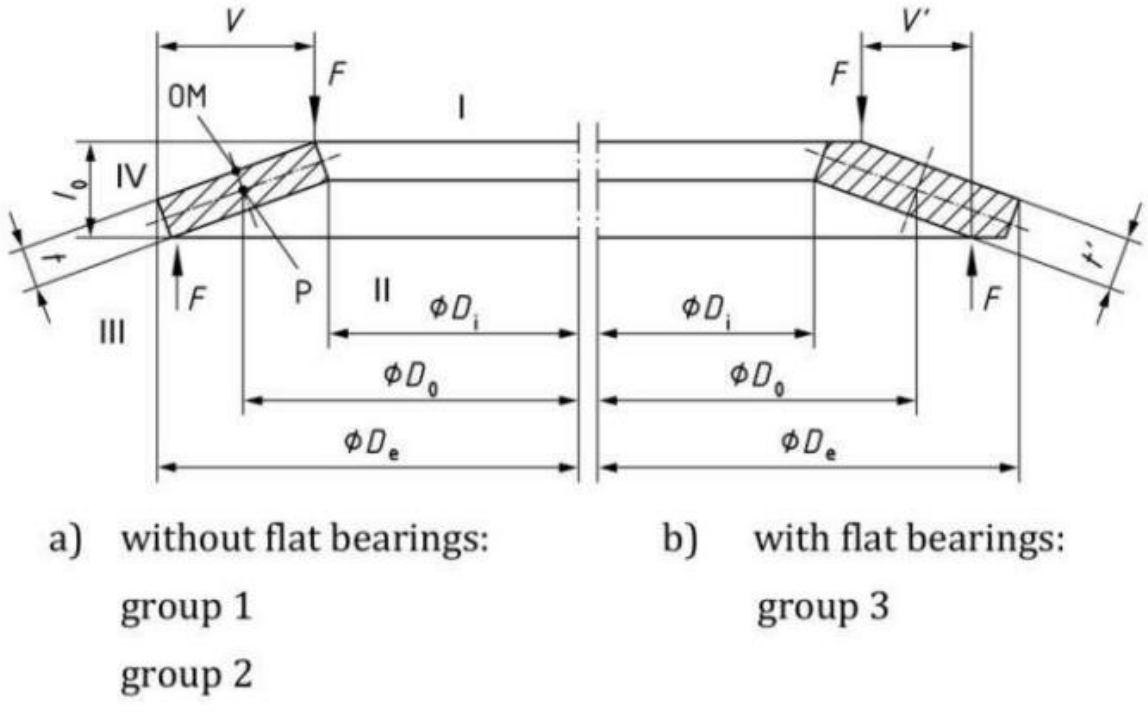


Figure 2-3 Single Disc Spring (sectional view), including the relevant points of loading

For disc springs without flat bearing surfaces, the standard distinguishes between Group 1 and Group 2 based on the magnitude of the reduced thickness ratio. Group 1-disc springs operate at lower reduced thickness ratios, while Group 2-disc springs cover an intermediate range, still

without the presence of flat bearing surfaces. In contrast, Group 3-disc springs include flat bearing surfaces at the inner and outer edges and are characterized by higher reduced thickness ratios. The inclusion of flat bearing surfaces modifies the contact conditions during loading and unloading and affects the internal stress distribution within the spring cross-section.

The influence of flat bearing surfaces and geometric group classification on the disc spring configuration is illustrated in Figure 2-3, which compares disc springs without flat bearing surfaces to disc springs with flat bearing surfaces. In addition to dimensional representation, this figure also identifies standardized stress evaluation points, commonly denoted as points I, II, III, IV, and the OM point.

These stress evaluation points correspond to critical regions within the disc spring where tensile stresses may develop depending on the applied load and geometric ratios. Among these locations, the OM point is of particular importance, as it is used in the standard as a reference point for design stress verification under both static and cyclic loading conditions. The identification of these points is therefore essential for the correct application of the stress evaluation procedures defined in BS EN 16984:2016.

The correct identification of the disc spring geometric group and the associated dimensional parameters is a prerequisite for applying the analytical formulations for load–deflection behaviour and stress evaluation provided in BS EN 16984:2016. For this reason, geometric classification according to BS EN 16983:2016 constitutes the first mandatory step in the disc spring design methodology adopted in this study.

### 2.4.2. Deflection Factors and Load-Deflection Formulation

The load–deflection behaviour of disc springs is formulated in BS EN 16984:2016 using a set of dimensionless geometric factors that relate the applied axial deflection to the resulting spring load [3].

Before the axial spring load can be calculated, the standard introduces a diameter ratio defined as

$$\delta = \frac{D_e}{D_i} \tag{2.4.2.1}$$

This ratio captures the influence of spring geometry on stiffness and stress distribution and is used to determine a series of dimensionless deflection factors.

Based on the diameter ratio $\delta$, the deflection factors $K_1$, $K_2$, $K_3$, and $K_4$are calculated according to the analytical expressions given in BS EN 16984:2016. These factors account for the combined effects of geometry and elastic behaviour and are expressed as

$$K_1 = \frac{1}{\pi}\left(\frac{\delta - 1}{\delta}\right)^2 \left(\frac{\delta + 1}{\delta - 1} - \frac{2}{\ln \delta}\right) \tag{2.4.2.2}$$

$$K_2 = \frac{6}{\pi}\left(\frac{\delta - 1}{\ln \delta}\right) \tag{2.4.2.3}$$

$$K_3 = \frac{3}{\pi}\left(\frac{\delta - 1}{\ln \delta}\right) \tag{2.4.2.4}$$

$$K_4 = \sqrt{\frac{C_1}{2} + \left(\frac{C_1}{2}\right)^2 + C_2} \tag{2.4.2.5}$$

Where:

$$C_1 = \frac{\left(\frac{t'}{t}\right)^2}{\left(\frac{1}{4} \times \frac{l_0}{t} - \frac{t'}{t} + \frac{3}{4}\right) \times \left(\frac{5}{8} \times \frac{l_0}{t} - \frac{t'}{t} + \frac{3}{8}\right)} \quad (2.4.2.6)$$

$$C_2 = \frac{C_1}{\left(\frac{t'}{t}\right)^3}\left[\frac{5}{32}\left(\frac{l_0}{t} - 1\right)^2 + 1\right] \quad (2.4.2.7)$$

Using these factors, the spring load $F_p$ as a function of deflection $s$ is expressed by:

$$F_p = \frac{E}{1 - v^2} \times \frac{t^4}{K_1 \times D_e^2} \times K_4^2 \times \frac{s}{t}\left[K_4^2 \times \left(\frac{h_0}{t} - \frac{s}{t}\right)\left(\frac{h_0}{t} - \frac{s}{2t}\right) + 1\right] \quad (2.4.2.8)$$

Where $F_p$ is the single Belleville Spring force, $E$ is the elastic modulus, $v$ is the Poisson's ratio, and $s$ is the deflection of a single Belleville Spring.

This expression shows that the axial load is a nonlinear function of deflection, reflecting the characteristic behaviour of disc springs.

The nonlinear nature of the load–deflection relationship implies that the stiffness of a disc spring varies throughout the compression range. At small deflections, the spring stiffness generally increases, while at higher deflections the slope of the curve may decrease depending on the geometric configuration. This behaviour is particularly relevant for applications involving preload definition, as it requires careful selection of the operating deflection range.

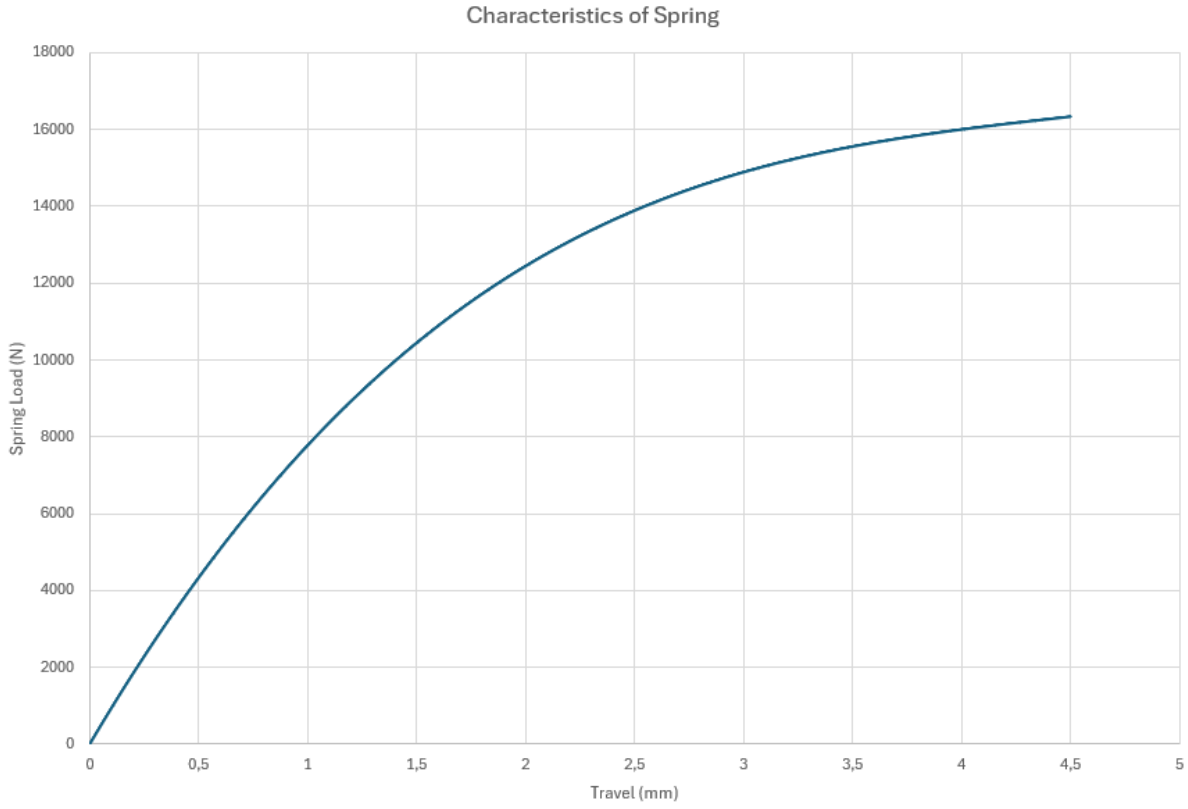


Figure 2-4 Sample Load/Deflection curve of single Belleville Spring

A representative load–deflection characteristic curve illustrating this non-linear behaviour for a single disc spring is presented in Figure 2-4.

### 2.4.3. Design Stress

In addition to the load–deflection behaviour, the structural integrity of a disc spring must be verified by evaluating the stresses generated under axial compression. BS EN 16984:2016 provides analytical expressions for calculating nominal tensile stresses at standardized locations within the disc spring cross-section, which are used for design verification purposes [3]. The definition and physical location of these stress evaluation points, denoted as points I, II, III, IV, and OM, are given in BS EN 16983:2016 and were previously illustrated in Section 2.4.1 [2].

The stresses calculated using the standard formulations are nominal design stresses and are expressed as functions of disc spring geometry, material properties, and axial deflection. These stresses represent idealized values and do not include residual stresses introduced during manufacturing or heat treatment. Nevertheless, they provide a consistent and conservative basis for disc spring design when applied according to the standard methodology [2,3].

For a disc spring subjected to an axial deflection $s$, the nominal tensile stresses at the standardized locations I, II, III, and IV are given by the following expressions [3]:

$$\sigma_I = -\frac{4E}{1-v^2} \times \frac{t^2}{K_1 \times D_e^2} \times K_4 \times \frac{s}{t}\left[K_4 \times K_2\left(\frac{h_0}{t} - \frac{s}{2t}\right) + K_3\right] \quad (2.4.3.1)$$

$$\sigma_{II} = -\frac{4E}{1-v^2} \times \frac{t^2}{K_1 \times D_e^2} \times K_4 \times \frac{s}{t}\left[K_4 \times K_2\left(\frac{h_0}{t} - \frac{s}{2t}\right) - K_3\right] \quad (2.4.3.2)$$

$$\sigma_{III} = -\frac{4E}{1-v^2} \times \frac{t^2}{K_1 \times D_e^2} \times K_4 \times \frac{1}{\delta} \times \frac{s}{t}\left[K_4 \times (K_2 - 2K_3) \times \left(\frac{h_0}{t} - \frac{s}{2t}\right) + K_3\right] \quad (2.4.3.3)$$

$$\sigma_{IV} = -\frac{4E}{1-v^2} \times \frac{t^2}{K_1 \times D_e^2} \times K_4 \times \frac{1}{\delta} \times \frac{s}{t}\left[K_4 \times (K_2 - 2K_3) \times \left(\frac{h_0}{t} - \frac{s}{2t}\right) - K_3\right] \quad (2.4.3.4)$$

Among these locations, the OM point is of particular importance and is treated separately as the governing design stress criterion in disc spring applications. The nominal tensile stress at the OM point is calculated using the expression defined in BS EN 16984:2016 [3]:

$$\sigma_{OM} = -\frac{4E}{1-v^2} \times \frac{t^2}{K_1 \times D_e^2} \times K_4 \times \frac{s}{t} \times \frac{3}{\pi} \quad (2.4.3.5)$$

Where $\sigma_I$, $\sigma_{II}$, $\sigma_{III}$, $\sigma_{IV}$, and $\sigma_{OM}$ represent the design stresses at the points designated I, II, III, IV, and OM, respectively

Similarly, stresses at other critical points (often denoted as I, II, III, IV) are also evaluated using the corresponding standard expressions:

Although stresses are evaluated at multiple locations, the design verification is primarily performed using the OM stress. According to BS EN 16983:2016 and BS EN 16984:2016, safe operation of a disc spring requires that the maximum calculated OM stress over the entire working deflection range remains lower than the tensile strength $R_m$of the selected spring material [2,3].

This design criterion is expressed as

$$\sigma_{OM,max} \leq R_m \quad (2.4.3.6)$$

Where $R_m$ represents the tensile strength of the Belleville Spring.

$R_m$ is obtained from the applicable material standard EN 10132-4 and the corresponding heat treatment specification defined in DIN 17221 [4,5]. Compliance with this condition ensures that the disc spring operates within the permissible stress limits recommended by the standards.

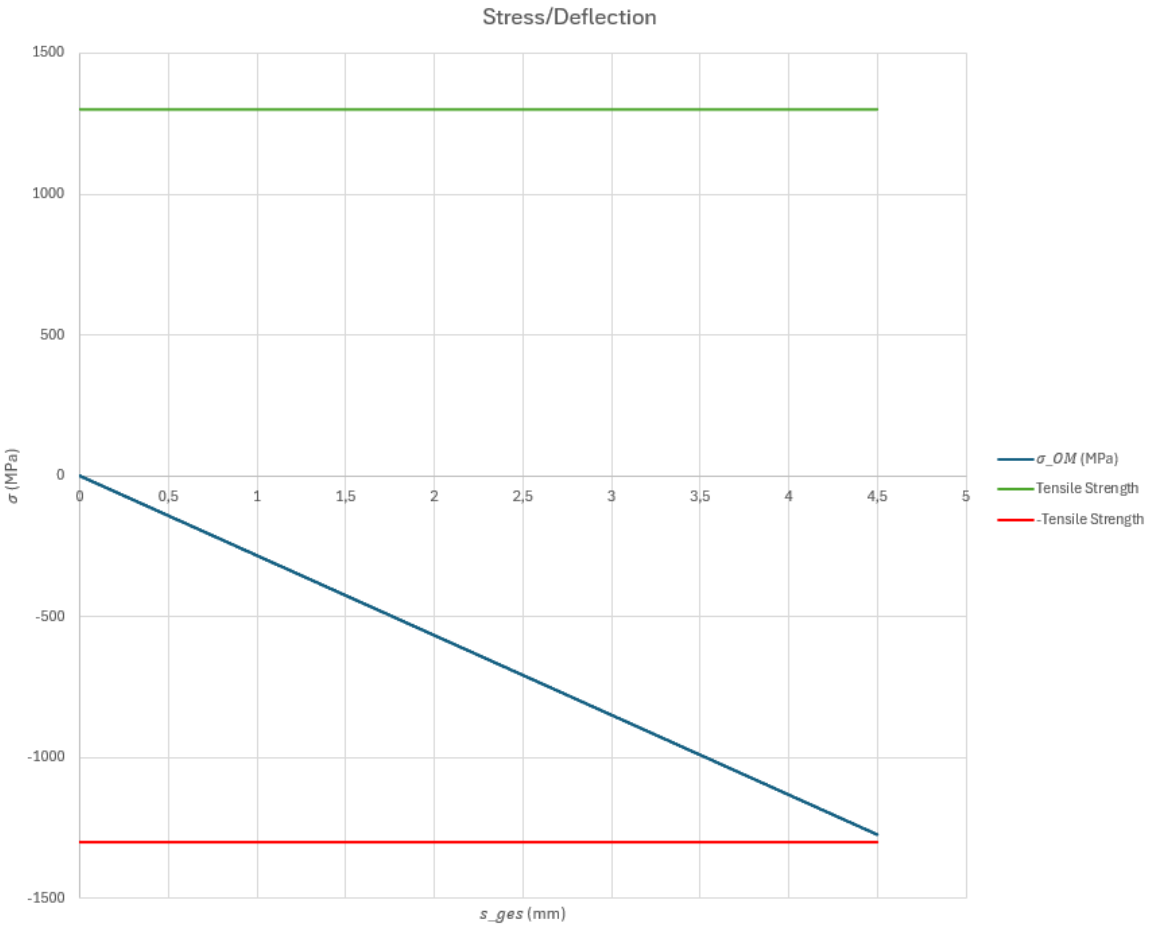


Figure 2-5 Sample calculated stresses σ_OM versus deflection, with tensile strength R_mindicated

The variation of the calculated stresses (including the critical OM stress) as a function of deflection is illustrated in Figure 2-5.

### 2.4.4. Stacking of Disc Springs

In practical applications, a single disc spring is often insufficient to simultaneously meet the required axial force and working deflection. For this reason, disc springs are commonly combined into stacks arranged in series, in parallel, or in mixed configurations. BS EN 16984:2016 provides analytical relationships that describe how the force–deflection behaviour of a single disc spring is transformed when multiple springs are stacked together [3].

When disc springs are stacked in parallel, all springs experience the same deflection, while the total axial force generated by the stack increases in proportion to the number of springs arranged in parallel. This configuration is typically used when a high axial force is required within a limited deflection range. For a parallel stack consisting of $n$ identical disc springs, the equivalent axial force $F_p$is expressed as

$$F_a = n \times F_p \tag{2.4.4.1}$$

By contrast, when disc springs are stacked in series, the same axial force acts on each spring, while the total deflection of the stack increases in proportion to the number of springs arranged in series. This configuration is preferred when a larger working deflection is required without

increasing the axial force level. For a series stack consisting of $i$ identical disc springs, the equivalent deflection $s_s$is given by

$$s_s = i \times s \tag{2.4.4.2}$$

In this configuration, the equivalent axial force remains equal to the force generated by a single spring.

In many engineering applications, disc springs are arranged in combined series–parallel stacks to achieve a tailored force–deflection characteristic. In such cases, groups of springs are first arranged in parallel to increase force capacity, and these parallel groups are then stacked in series to increase the total working deflection. The resulting force–deflection behaviour of the complete stack can be obtained by applying the parallel and series relations sequentially, as defined in BS EN 16984:2016 [3]. The visual representation of these stacking configurations (parallel, series, and combined) and their effect on the force–deflection curve is shown in Figure 2-6.

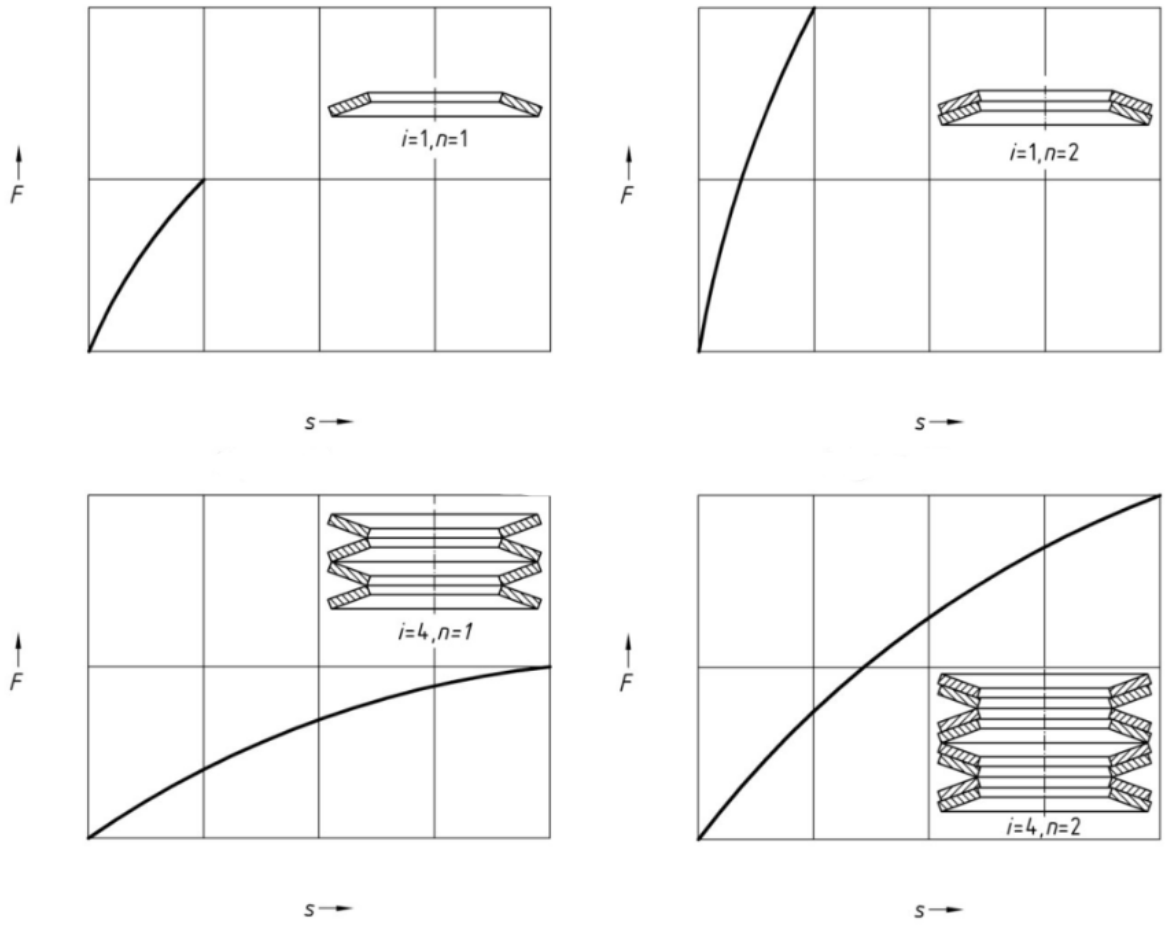


Figure 2-6 Variations in load/deflection curves as a function of Belleville Spring stacking

In addition to force and deflection, the overall free height of the stacked disc spring assembly must be considered to ensure compatibility with the available installation space. For a stack consisting of $i$ springs in series, $L_0$can be approximated as

$$L_0 = i[l_0 + (n-1)t] \tag{2.4.4.3}$$

This geometric relation is used to verify that the assembled spring stack can be accommodated within the axial space constraints of the dropbox housing.

In this study, the stacking relations defined above were integrated into the iterative calculation procedure described in the following section. By combining the load–deflection behaviour of a single disc spring with the stacking equations, the axial preload force generated by the complete disc spring assembly could be evaluated as a function of total stack deflection and directly linked to the wet clutch torque capacity.

### 2.4.5. Iterative Spring Calculation Procedure and Operating Point Selection

Due to the nonlinear load–deflection behaviour of disc springs and the coupled relationship between spring force and clutch torque capacity, a direct analytical solution for the operating point is not practical. Instead, the disc spring system in this study was evaluated using an iterative calculation procedure implemented in a spreadsheet environment. This approach allows the continuous tracking of spring force, stress levels, and clutch torque capacity as functions of spring deflection.

In the adopted methodology, the disc spring is compressed incrementally starting from the unloaded state. At each incremental deflection step, the axial spring force is calculated using the load–deflection formulation defined in Section 2.4.2, while the corresponding stresses are evaluated using the stress equations presented in Section 2.4.3. The stacking relations described in Section 2.4.4 are applied simultaneously to obtain the equivalent force and deflection of the complete spring assembly. This procedure ensures that the mechanical behaviour of the stacked disc spring system is consistently represented throughout the entire compression range.

A small deflection increment was selected to provide sufficient resolution in the force–deflection and stress–deflection curves. In this study, an incremental step size of 0.001 mm was used, which allows the gradual evolution of spring characteristics to be captured with high accuracy. At each deflection increment, the resulting axial force generated by the disc spring stack is used as the normal force acting on the wet clutch friction disc pack. This normal force is then employed to evaluate the corresponding clutch torque capacity using the formulation established in the wet clutch analysis.

By iterating over the full deflection range, a continuous mapping between disc spring deflection, axial preload force, and transmitted clutch torque is obtained. This mapping enables the identification of the operating deflection at which the generated clutch torque meets or safely exceeds the required dropbox output torque determined from the duty cycle analysis. At the same time, the stress values calculated at this operating point are verified to remain within the permissible limits defined by the material properties and applicable standards. The overall logic of this iterative spring–clutch matching procedure is summarized in the flowchart provided in Figure 2-7.

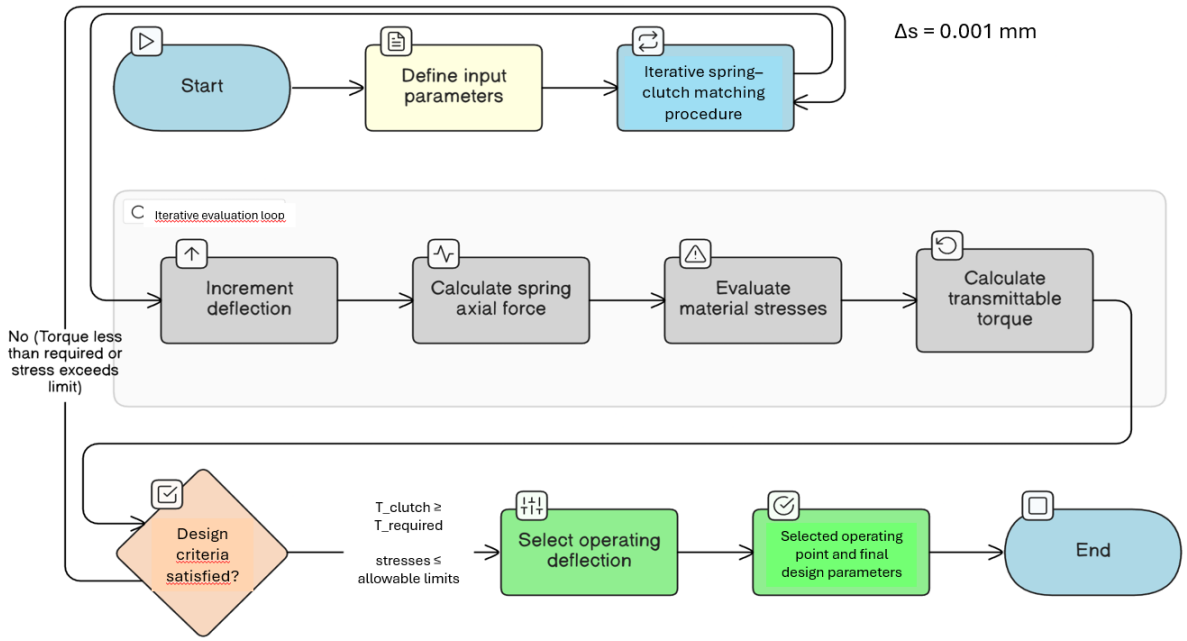


Figure 2-7 The iterative spring–clutch matching procedure used to determine the operating deflection that satisfies both torque transmission and stress constraints

The iterative procedure described in this section provides a transparent and systematic framework for selecting the disc spring operating point. The numerical application of this methodology, including the determination of the final operating deflection, corresponding axial preload force, and associated stress levels, is presented in the following subsection.

### 2.4.6. Calculations

This section presents the numerical implementation of the disc spring model defined in Sections 2.4.1–2.4.5. The calculations were carried out using the standardized load–deflection and stress formulations for disc springs given in BS EN 16984:2016 [3], while the geometric definition and group classification were taken from BS EN 16983:2016 [2]. The purpose of the procedure is to determine (i) the spring preload deflection required to provide the target clutch clamp load and (ii) the corresponding stress level within the usable operating range of the spring stack.

Table 2-6 Belleville Spring Physical Properties

| | | |
|---|---|---|
| $D_e$ | 124,6 | mm |
| $D_i$ | 64 | mm |
| $t$ | 2,2 | mm |
| $t'$ | 2,2 | mm |
| $l_0$ | 8 | mm |
| $E$ | 210000 | MPa |
| $v$ | 0,3 | |
| $h_o$ | 5,8 | mm |
| $n$ | 2 | |
| $i$ | 2 | |
| $s_{s,max}$ | 11,6 | mm |
| $L_0$ | 20,4 | mm |

Table 2-6 summarizes the physical parameters of the disc springs physically available in the investigated dropbox system. These values correspond to the measured spring geometry and the assembled stack configuration used in the drivetrain unit. In the present configuration, flat bearing surfaces are not included, and the spring is treated as a disc spring without flat bearings according to the group definition in BS EN 16983:2016 [2]. The stack arrangement was selected as $n = 2$ springs in parallel and $i = 2$ springs in series in order to satisfy the available axial installation space and to fill the internal clearance of the clutch–piston region. Although the section view of the dropbox assembly (see **Hata! Başvuru kaynağı bulunamadı.**) appears highly compact, a machined piston with internal material removal was implemented in the test hardware to accommodate the required stack length.

The elastic properties used in the analytical model were taken as $E = 210\,000$MPa and $\nu = 0.30$, which are taken from open sources. The maximum permitted deflection for the available spring set was defined as $s_s = 11.6$ mm, consistent with the measured free geometry and the practical compression limit of the component set.

The numerical evaluation was performed iteratively by increasing the spring deflection in fixed increments of $\Delta s = 0.001$ mm. At each increment, the spring axial force was computed using the load–deflection relations provided in BS EN 16984:2016 [3] (see the equations introduced in Section 2.4.2). In the same loop, the stress state was evaluated using the standardized stress expressions for the defined locations on the disc spring cross-section (see Section 2.4.3) [3]. Finally, the transmittable wet clutch torque corresponding to the calculated axial clamp load was determined using the clutch torque capacity relation already introduced in Section 2.3 (wet clutch model based on friction interfaces and mean friction radius). This creates a direct link between disc spring compression, clamp force, stress level, and torque capacity.

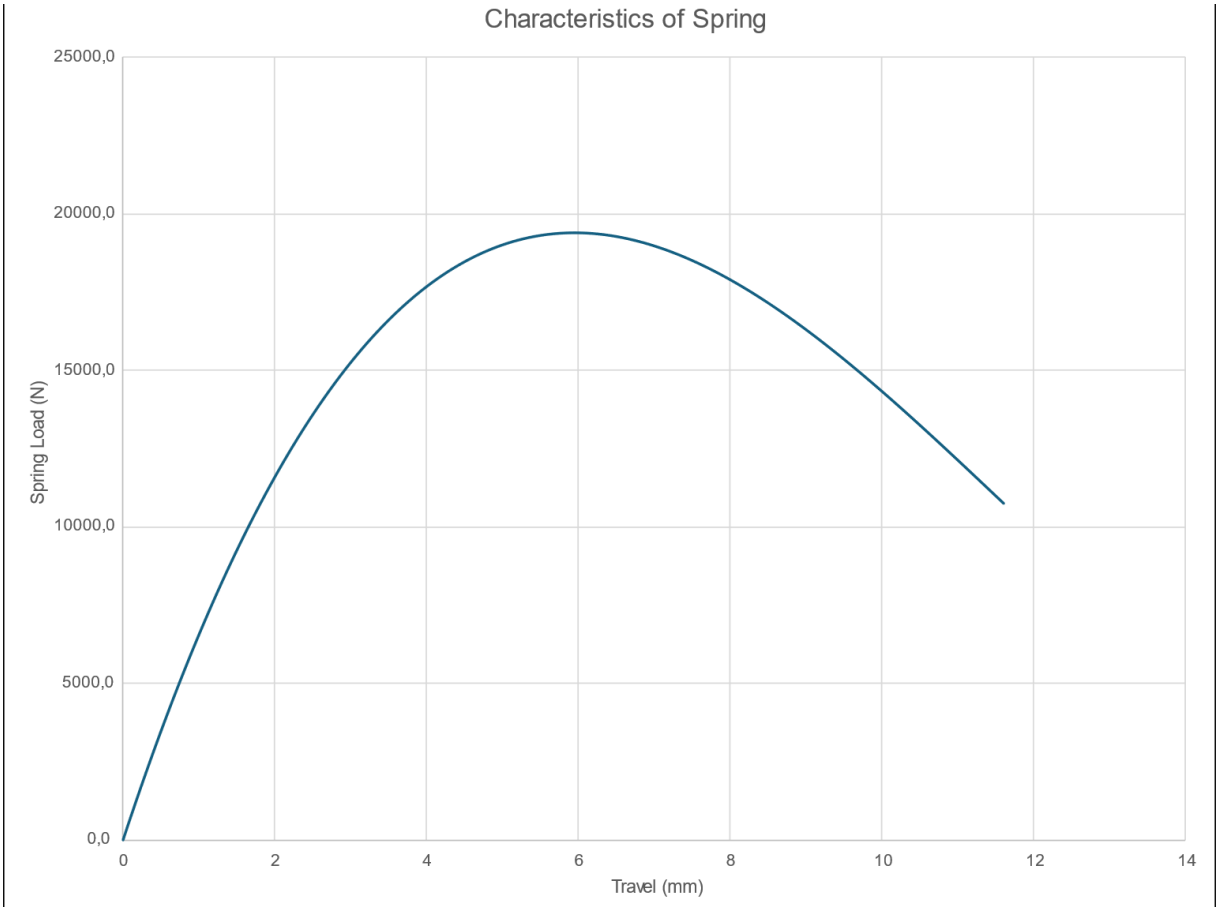


Figure 2-8 Characteristics of Spring (Spring Load vs Travel Distance)

Figure 2-8 shows the measured/implemented spring characteristic over the evaluated deflection range. The curve exhibits a non-monotonic behaviour at large deflections, where the axial force reaches a peak value and then decreases with further compression. This behaviour is a consequence of the non-standard spring geometry of the available components and differs from the strictly increasing trend typically expected from standard disc springs. In the present dataset, the maximum spring force is $F_{\max} = 19\,395\text{N}$ at a deflection of $s = 5.948\text{mm}$. However, it is important to emphasize that the operating region of the dropbox clutch does not utilize the spring stack in this non-monotonic range. The clutch preload requirement is achieved at a very small deflection compared to the peak location. Moreover, considering the maximum piston stroke required for disengagement (4×2 transition), the total spring compression during operation is expected to remain around $\sim 1.6\text{mm}$, which is significantly below the region where the characteristic deviates (approximately 6 mm and beyond). Therefore, the design is evaluated and validated only within the initial monotonic region of the force–deflection curve that is actually used by the system.

Table 2-7 Iterative calculation results

| $s_s$ (mm) | $F_p$ (N) | $\sigma_{OM}$ (MPa) | $\sigma_I$ (MPa) | $\sigma_{II}$ (MPa) | $\sigma_{III}$ (MPa) | $\sigma_{IV}$ (MPa) | $T_f$ (Nm) |
|---|---|---|---|---|---|---|---|
| 0,165 | 1193,2 | -15,1 | -71,4 | -28,5 | 43,0 | 21,0 | 706,4 |
| 0,166 | 1200,3 | -15,2 | -71,8 | -28,7 | 43,3 | 21,1 | 710,6 |
| 0,167 | 1207,4 | -15,3 | -72,2 | -28,8 | 43,5 | 21,2 | 714,8 |
| 0,168 | 1214,5 | -15,4 | -72,7 | -29,0 | 43,8 | 21,4 | 719,0 |
| 0,169 | 1221,6 | -15,5 | -73,1 | -29,2 | 44,1 | 21,5 | 723,2 |
| 0,170 | 1228,7 | -15,5 | -73,5 | -29,3 | 44,3 | 21,6 | 727,4 |
| 0,171 | 1235,8 | -15,6 | -74,0 | -29,5 | 44,6 | 21,7 | 731,6 |
| 0,172 | 1242,9 | -15,7 | -74,4 | -29,7 | 44,8 | 21,9 | 735,8 |
| 0,173 | 1249,9 | -15,8 | -74,8 | -29,9 | 45,1 | 22,0 | 740,0 |
| 0,174 | 1257,0 | -15,9 | -75,3 | -30,0 | 45,4 | 22,1 | 744,2 |
| 0,175 | 1264,1 | -16,0 | -75,7 | -30,2 | 45,6 | 22,2 | 748,4 |
| 0,176 | 1271,2 | -16,1 | -76,1 | -30,4 | 45,9 | 22,4 | 752,6 |
| 0,177 | 1278,3 | -16,2 | -76,5 | -30,5 | 46,1 | 22,5 | 756,8 |
| 0,178 | 1285,3 | -16,3 | -77,0 | -30,7 | 46,4 | 22,6 | 761,0 |
| 0,179 | 1292,4 | -16,4 | -77,4 | -30,9 | 46,6 | 22,8 | 765,2 |
| 0,180 | 1299,5 | -16,5 | -77,8 | -31,1 | 46,9 | 22,9 | 769,4 |
| 0,181 | 1306,6 | -16,5 | -78,3 | -31,2 | 47,2 | 23,0 | 773,5 |
| 0,182 | 1313,6 | -16,6 | -78,7 | -31,4 | 47,4 | 23,1 | 777,7 |
| 0,183 | 1320,7 | -16,7 | -79,1 | -31,6 | 47,7 | 23,3 | 781,9 |
| 0,184 | 1327,8 | -16,8 | -79,6 | -31,7 | 47,9 | 23,4 | 786,1 |
| 0,185 | 1334,8 | -16,9 | -80,0 | -31,9 | 48,2 | 23,5 | 790,3 |
| 0,186 | 1341,9 | -17,0 | -80,4 | -32,1 | 48,5 | 23,6 | 794,5 |
| 0,187 | 1348,9 | -17,1 | -80,8 | -32,2 | 48,7 | 23,8 | 798,6 |
| 0,188 | 1356,0 | -17,2 | -81,3 | -32,4 | 49,0 | 23,9 | 802,8 |
| 0,189 | 1363,1 | -17,3 | -81,7 | -32,6 | 49,2 | 24,0 | 807,0 |
| 0,190 | 1370,1 | -17,4 | -82,1 | -32,8 | 49,5 | 24,1 | 811,2 |
| 0,191 | 1377,2 | -17,5 | -82,6 | -32,9 | 49,8 | 24,3 | 815,3 |
| 0,192 | 1384,2 | -17,6 | -83,0 | -33,1 | 50,0 | 24,4 | 819,5 |
| 0,193 | 1391,3 | -17,6 | -83,4 | -33,3 | 50,3 | 24,5 | 823,7 |
| 0,194 | 1398,3 | -17,7 | -83,8 | -33,4 | 50,5 | 24,6 | 827,9 |
| 0,195 | 1405,4 | -17,8 | -84,3 | -33,6 | 50,8 | 24,8 | 832,0 |

A representative excerpt of the iterative computation table is presented in Table 2-7 to illustrate the incremental procedure and the resulting evolution of axial force, stress values, and clutch torque capacity with deflection. The complete dataset is not included in the main report due to its large size (approximately 9000 rows). Instead, the full iterative results are provided as a supplementary Excel (.xlsx) file accompanying this report.

Based on the duty-cycle-based design condition identified earlier, the required dropbox output torque was taken as $T_{\text{req}} = 767.64\text{Nm}$ (see Section 2.3.1). By scanning the iterative results, the preload deflection that provides the closest matching torque capacity within the allowable stress limits was selected as the operating preload. For the critical load case considered, the required spring preload deflection was found as $s_{\text{preload}} = 0.180$ mm, which produces an axial clamp

force of $F_{\text{preload}} = 1299.48\text{N}$. This preload force constitutes the design clamp load used for subsequent verification steps and for the hydraulic disengagement pressure calculation discussed in the following sections.

### 2.4.7. Material Selection and Heat Treatment

The material verification of the disc spring was carried out based on the stress results obtained from the numerical calculations presented in Section 2.4.6. In disc spring design, the governing stress location is defined at the OM point, which corresponds to the most critical region of tensile or compressive stress depending on the spring geometry and loading condition, as specified in BS EN 16984:2016 [3]. Therefore, the verification of material suitability was performed by comparing the calculated maximum stress at the OM location with the tensile strength of the selected spring steel.

For the operating preload deflection selected in the design, the maximum stress at the OM point was calculated as approximately -1060 MPa. The negative sign indicates that the stress state at the OM location is compressive, which is consistent with the loading condition of the disc spring under axial preload. This distinction is important, as compressive stresses are generally less critical than tensile stresses with respect to crack initiation and fatigue failure in spring steels [3].

The spring material used in the investigated system is 50CrV4 spring steel, whose tensile strength was taken as $R_m = 1200$-1800 MPa, based on standard material specifications for quenched and tempered spring steels defined in EN 10132-4 and the associated heat treatment conditions specified in DIN 17221 [4,5]. In this study, the lower bound of this range (1200 MPa) was conservatively adopted as the reference tensile strength for design verification. This approach ensures that the stress assessment remains on the safe side and does not rely on optimistic material assumptions. This tensile strength represents the upper allowable stress level used as a design reference in disc spring verification procedures.

A direct comparison between the calculated OM stress and the material tensile strength shows that the absolute value of the maximum compressive stress remains below the tensile strength limit of the material. Consequently, the disc spring operates within the allowable stress range defined by the relevant standards, and no material yielding or permanent deformation is expected under the selected preload condition.

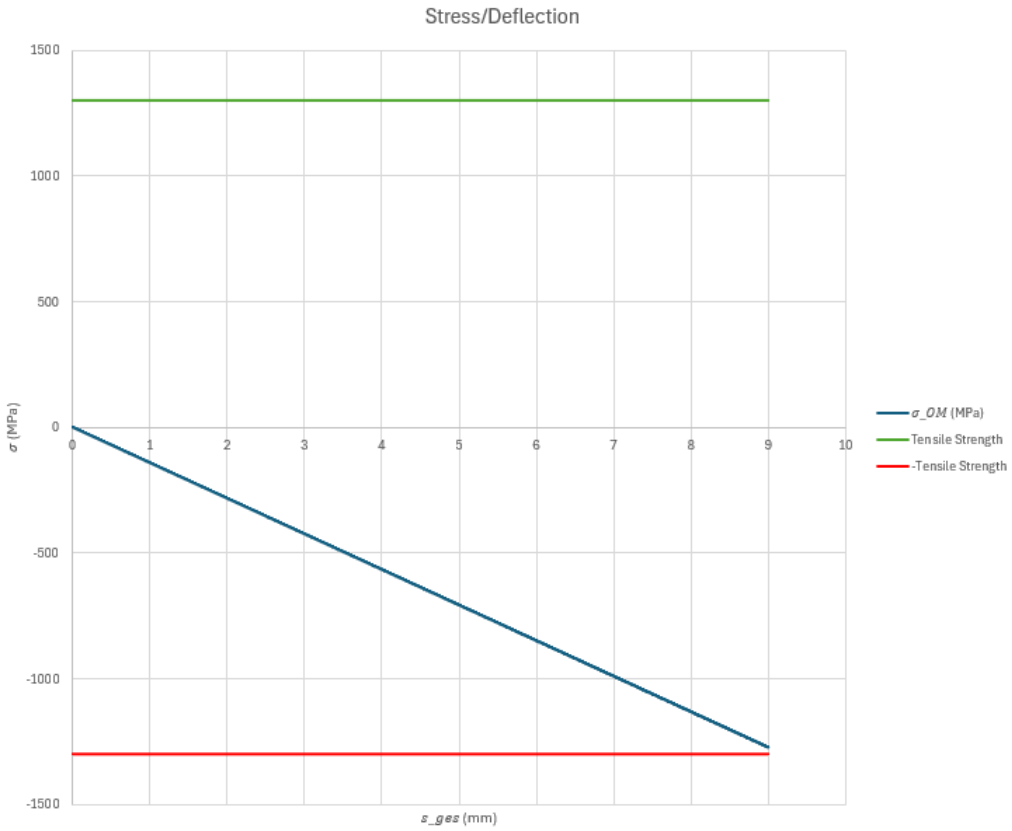


Figure 2-9 Stress/Deflection Curve

Figure 2-9 summarizes the calculated maximum OM stress and the corresponding tensile strength of the spring material. This comparison confirms that the selected spring operates with an adequate safety margin within the elastic regime for the intended operating range.

It should also be noted that the operating preload deflection is significantly lower than the deflection level at which non-monotonic behaviour is observed in the spring characteristic curve. As a result, the stress verification presented here corresponds exclusively to the initial monotonic region of the force–deflection response, which is the only region utilized during normal operation and during the hydraulic disengagement process. This further supports the suitability of the selected material for the disc spring application considered in this study.

It should be noted that the spring characteristic curve provided in this study extends beyond the strictly defined standard operating region and includes stress evaluations at higher deflection levels. Although the force–deflection response becomes non-monotonic beyond the peak load point, the calculated stress values at the OM location continue to increase in a stable and continuous manner and remain within acceptable material limits. Therefore, the stress evaluation is not restricted solely to the initial monotonic region but also demonstrates that the spring material maintains structural integrity even when operating near or beyond the conventional standard boundaries.

### 2.5. Hydraulic Pressure Requirement for 4×2 Mode Switching

In order to switch the drivetrain from 4×4 to 4×2 mode, the wet clutch pack inside the dropbox must be disengaged by removing the clamp load generated by the preloaded disc spring stack. This is achieved by applying hydraulic pressure to an annular piston, which produces an axial

force acting against the spring preload. The minimum pressure requirement is determined by ensuring that the piston force is at least equal to the spring force at the disengagement stroke.
The effective piston area is calculated as the difference between the outer and inner circular areas:

$$A_p = \frac{\pi}{4}\left(D_{o,p}^2 - D_{i,p}^2\right) \quad (2.5.1)$$

Where $A_p$ is the effective piston area, and $D_{o,p}$ and $D_{i,p}$ represent the outer and inner diameters of the piston, respectively.
The piston force generated by a given hydraulic pressure is expressed as:

$$F_h = P \times A_p \quad (2.5.2)$$

Where $F_h$ is the piston force required to bypass the preload, and $P$ is the required piston pressure.
To disengage the clutch, the following condition must be satisfied:

$$F_h \geq F_p \quad (2.5.3)$$

Accordingly, the minimum hydraulic pressure required to overcome the spring preload becomes:

$$P_{min} = \frac{F_P}{A_p} \quad (2.5.4)$$

Table 2-8 Geometrical Specifications for Piston

| | | |
|---|---|---|
| $D_{o,p}$ | 120 | mm |
| $D_{i,p}$ | 55 | mm |
| Max. Piston Stroke | 1,45 | mm |
| Spring Preload and Piston Stroke Distance | 1,630 | mm |

In this study, the total piston travel required for disengagement was defined as the sum of the maximum piston stroke and the additional displacement needed to fully bypass the spring preload. The maximum piston stroke was taken as 1.45 mm, while the total required travel (spring preload plus piston stroke distance) was 1.670 mm, consistent with the assembly-based stroke definition.

Table 2-9 Results

| | | |
|---|---|---|
| $F_h$ | 9901,2 | N |
| $P$ | 11,08 | Bar |

Based on the spring force corresponding to this travel, the preload bypass force was taken as 9901.2 N. Substituting this value into the pressure equation yields a required hydraulic pressure of 11.08 bar. This pressure level represents the minimum theoretical pressure to guarantee clutch disengagement under the investigated operating condition and was later used as the reference input for evaluating the 4×2 switching performance of the system.

### 2.6. Drag Torque Analysis

During the transition from 4×4 to 4×2 operation, the wet clutch inside the dropbox is hydraulically disengaged, allowing relative motion between the friction and separator discs while they remain immersed in ATF (Automatic Transmission Fluid). Ideally, no torque should be transmitted in this disengaged state. However, due to viscous shear effects within the ATF

present in the inter-disc clearance, a resistive torque known as drag torque inevitably develops. This drag torque constitutes a parasitic loss in the drivetrain and must be evaluated to assess its influence on system performance and mode-switching reliability.

The generation of drag torque in open multi-disc wet clutches has been widely investigated in the literature. It is well established that drag torque originates from three distinct mechanisms: (i) viscous shear within a continuous ATF film, (ii) viscous effects associated with a ruptured or partially cavitated ATF film, and (iii) shear and momentum transfer due to an ATF mist film formed after film rupture [7,8]. Experimental and analytical studies consistently indicate that the dominant contribution to drag torque arises from the continuous ATF film, while the effects of the ruptured film and mist regime are significantly smaller, particularly at moderate rotational speeds.

$$T_d = T_{fa} + T_{ra} + T_{rm} \tag{2.6.1}$$

Where $T_d$ represents the total drag torque, $T_{fa}$ is the torque due to shear of ATF in the continuous section, $T_{ra}$ is the torque due to shear of ATF in the ruptured section weighted by a wetted fraction, and $T_{rm}$is the torque due to shear of the mist film in the ruptured section.

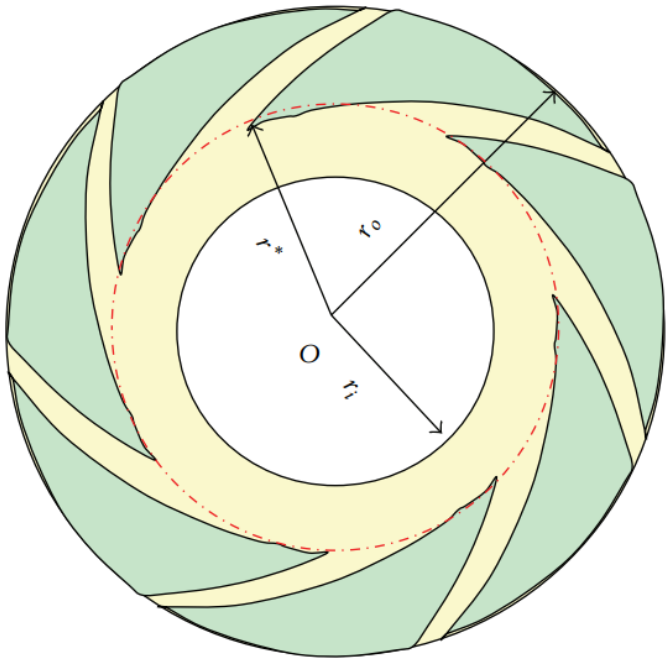


Figure 2-10 Schematic of the film shape, yellow and green portions represent the ATF and the mist film, respectively

A schematic representation of the friction interface, distinguishing between the continuous ATF film and the mist region involved in drag torque generation, is depicted in Figure 2-10.

Although the presence and physical relevance of the ruptured and mist regimes are acknowledged, a conservative modelling approach is adopted in the present study. The entire friction interface is assumed to operate under a fully flooded, continuous ATF film condition. This assumption intentionally neglects the reduced drag torque contributions associated with the ruptured and mist regimes and therefore yields an upper-bound estimate of drag torque. By following this approach, the drag torque calculation is biased toward safety, ensuring that potential parasitic effects are not underestimated. If the drag torque calculated under this

conservative assumption remains sufficiently small relative to the transmitted torque levels, it may be confidently neglected in the overall system assessment.

Under the assumption of laminar flow and a uniform ATF film of thickness $h$ between two parallel rotating discs, the drag torque generated by viscous shear can be expressed as

$$T_{fa,single} = \frac{2\pi\mu_{ATF}\Delta w}{h}\int_{r_{i,f}}^{r_{o,f}} r^3\, dr \tag{2.6.2}$$

Where $\mu_{ATF}$ represents the dynamic viscosity of the ATF, $\Delta w$ is the relative angular speed between the two friction disk sets, $h$ is the inter-disk clearance of the friction discs, and $r_o$ and $r_i$represent the outer and inner radii of the friction disc, respectively.

Evaluating the integral yields

$$T_{fa,single} = \frac{\pi\mu_{atf}\Delta w}{2h}(r_o^4 - r_i^4) \tag{2.6.3}$$

For a multi-disc wet clutch, the total drag torque is obtained by multiplying the above expression by the number of active fluid shear interfaces present in the clutch pack.

$$T_d = T_{fa} = \frac{\pi\mu_{atf}\Delta w n_f}{2h}(r_o^4 - r_i^4) \tag{2.6.4}$$

The effective oil film thickness is governed by the axial separation of the discs in the disengaged state. In the present design, the total piston stroke is distributed symmetrically across the friction interfaces. Accordingly, the average inter-disc clearance is defined as

$$h = \frac{\text{Max. Piston Stroke}}{2N} \tag{2.6.5}$$

The drag torque calculation requires accurate ATF properties at the operating temperature of the dropbox. Based on thermal considerations of the transmission system, the nominal ATF working temperature is taken as 80℃. The temperature-dependent ATF properties, including dynamic viscosity, kinematic viscosity, and density, are summarized in Table 2-10, which is placed immediately after this paragraph.

Table 2-10 Properties of ATF

| Temp. [°C] | Dyn. Viscosity [MPa.s] | Kin. Viscosity [mm²/s] | Density [g/cm³] |
|---|---|---|---|
| 0 | 217,29 | 247,39 | 0,878 |
| 10 | 118,06 | 135,42 | 0,872 |
| 20 | 70,04 | 80,93 | 0,866 |
| 30 | 44,7 | 52,04 | 0,859 |
| 40 | 30,31 | 35,55 | 0,853 |
| 50 | 21,53 | 25,44 | 0,846 |
| 60 | 15,93 | 18,97 | 0,840 |
| 70 | 12,18 | 14,62 | 0,833 |
| 80 | 9,57 | 11,58 | 0,827 |
| 90 | 7,71 | 9,39 | 0,821 |
| 100 | 6,32 | 7,77 | 0,814 |

The relative angular velocity of the friction interfaces is determined from the engine operating conditions. At the maximum engine speed of 2300 rpm and an engine-to-dropbox entrance gear ratio of 33.6858, the corresponding angular velocity is used in the drag torque formulation. The inter-disc clearance calculated from the piston stroke and the number of friction discs is $h =$

0.0806 mm. Substituting the geometric parameters, ATF dynamic viscosity at 80℃, calculated clearance, and angular velocity into the continuous film drag torque equation yields a total drag torque of

$$T_d = 5.19\ Nm$$

To evaluate the significance of this value, the calculated drag torque is compared with the maximum engine output torque, which is approximately 560.5 Nm for the selected tractor configuration. This comparison is illustrated in Table 2-11, where the relative magnitude of the drag torque with respect to the engine torque and summary of this section is shown.

Table 2-11 Summarized table of drag torque

| | | |
|---|---|---|
| Working Temperature | 80 | °C |
| Gear Raito (Engine > Dropbox Enterence) | 33,69 | |
| h | 0,0806 | mm |
| Max Engine Torque | 560,54 | Nm |
| Engine Exit Revoulution | 2300 | rpm |
| Drag Torque | 5,19 | Nm |
| Percentage Difference | 0.93 | % |

The calculated drag torque corresponds to less than 5% of the maximum engine torque. In drivetrain and clutch system design practice, parasitic torques below this threshold are generally considered negligible. Given that the present analysis is based on a fully flooded continuous film assumption, the actual drag torque under operating conditions is expected to be equal to or lower than the calculated value.

Therefore, drag torque effects are deemed negligible for the hydraulically disengaged wet clutch system integrated into the dropbox and are not expected to influence the functional performance, hydraulic disengagement capability, or mode transition reliability of the 4×4 to 4×2 system.

# 3. RESULT & DISCUSSION

This chapter presents the consolidated findings obtained from both the analytical design calculations and the experimental validation tests. First, the key design outputs derived from the methodology described in the previous chapter—including the finalized spring preload, required hydraulic disengagement pressure, and estimated drag torque—are summarized in a tabulated format. Subsequently, the results from the physical experiments conducted on the dropbox assembly are reported, focusing on the hydraulic pressure threshold required to bypass the spring preload. The chapter concludes with a comparative analysis of the analytical predictions and the experimental observations to validate the accuracy of the design model and the reliability of the proposed clutch system.

## 3.1. Summary of Analytical Design Results

This section presents the analytical design results of the hydraulically actuated wet multi-disc clutch system in a structured and tabulated form. All results were obtained using the analytical formulations described in Chapter 2 and implemented through an iterative Excel-based calculation procedure. The tabulated presentation allows the key design outcomes to be directly assessed without requiring detailed examination of the preceding analytical derivations.

The primary design inputs, including Belleville Spring properties, friction disc characteristics, and duty cycle-based operating conditions, are summarized in Table 3-1, Table 3-2, and Table 3-3. These parameters form the basis of the clutch torque capacity and preload force calculations.

Table 3-1 Belleville Spring Properties

| | | |
|---|---|---|
| Material | 50 CrV 4 | |
| Geometrical Standard | BS EN 16983 - 2016 | |
| Heat Treatment | DIN 17 221 | |
| Material Standard | EN 10132-4 | |
| $D_e$ | 124,6 | mm |
| $D_i$ | 64 | mm |
| $t$ | 2,2 | mm |
| $t'$ | 2,2 | mm |
| $l_0$ | 8 | mm |
| $R_m$ | 1200 | MPa |
| $E$ | 210000 | MPa |
| $v$ | 0,3 | |
| $h_o$ | 5,8 | mm |
| $n$ | 2 | |
| $i$ | 2 | |
| $s_{s,max}$ | 11,6 | mm |
| $L_0$ | 20,4 | mm |

Table 3-2 Friction Disc Properties

| | | |
|---|---|---|
| $N$ | 9 | |
| $n_f$ | 18 | |
| $D_{o,f}$ | 133,35 | mm |
| $D_{i,f}$ | 100 | mm |
| $\mu$ | 0,14 | |
| $r_m$ | 58,73 | mm |

Table 3-3 Values from Duty Cycle

| Power at Wheel (kW) | Tractor Speed (km/h) | Min. Dropbox Output Torque (Nm) |
|---|---|---|
| 6,09 | 1,3 | 767,6 |

Using the parameters listed in Table 3-1,
Table 3-2, and
Table 3-3, the required torque capacity at the dropbox output was determined. The worst-case operating condition corresponds to a required dropbox output torque of 767.64 Nm. The

resulting axial preload force required to transmit this torque without slip, together with the associated spring deflection, is summarized in Table 3-4.

Table 3-4 Dropbox Torque and Spring Force

| | | |
|---|---|---|
| Dropbox Exit Torque | 767,64 | Nm |
| Spring Deflection | 0,180 | mm |
| Spring Force | 1299,48 | N |

The preload force listed in Table 3-4 is generated by a stacked Belleville spring configuration operating within its monotonic load–deflection region. Stress evaluation at the governing OM location confirmed that the maximum compressive stress remains below the conservative tensile strength limit of the spring material. The stress–deflection relationship and spring characteristic curve supporting this conclusion were previously presented in Chapter 2.

To enable disengagement of the clutch during the transition from 4×4 to 4×2 operation, a hydraulic piston was designed to overcome the spring preload force. The piston geometry and the resulting hydraulic pressure required to bypass the preload are summarized in Table 3-5.

Table 3-5 Piston Pressure (To Bypass Preload)

| | | |
|---|---|---|
| Piston Outer Diameter | 120 | mm |
| Piston Inner Diameter | 55 | mm |
| Max. Piston Stroke | 1,45 | mm |
| Spring Preload and Piston Stroke Distance | 1,630 | mm |
| Spring Force | 9901,2 | N |
| Required Pressure | 11,08 | Bar |

The calculated hydraulic pressure of approximately 11.3 bar is compatible with the hydraulic capabilities of the tractor transmission system, indicating that reliable disengagement can be achieved without exceeding system limits.

In the disengaged state, viscous shear within the ATF generates a drag torque between the friction interfaces. Adopting a conservative continuous film assumption at an operating temperature of 80 °C, the calculated drag torque and its comparison with the maximum engine torque are presented in Table 3-6.

Table 3-6 Drag Torque

| | | |
|---|---|---|
| Gear Raito (Engine > Dropbox Entrance) | 33,69 | |
| h | 0,0806 | mm |
| Max Engine Torque | 560,54 | Nm |
| Engine Exit Revolution | 2300 | rpm |
| Drag Torque | 5,19 | Nm |
| Percentage Difference | 0.93 | % |

As shown in Table 3-6, the drag torque represents less than 5% of the maximum engine torque. Therefore, drag torque effects are considered negligible for the present application and are not expected to influence the functional behaviour of the dropbox during 4×2 operation.
Overall, the results summarized in Tables 10-15 demonstrate that the required torque capacity, spring preload characteristics, hydraulic disengagement pressure, and drag torque behaviour are mutually consistent and satisfy the design objectives. These analytical findings provide a solid foundation for the experimental results and comparative discussion presented in the following section.

### 3.2. Experimental Results

An experimental study was conducted to determine the hydraulic pressure required to disengage the wet multi-disc clutch and enable the transition from 4×4 to 4×2 operation in the dropbox assembly. The primary objective of the experiment was to identify the pressure level at which torque transmission between the input and output shafts is eliminated due to the release of the spring preload.
The experimental setup consisted of a hydraulic power unit, the assembled dropbox housing, and a pressure measurement system. Hydraulic pressure was supplied to the dropbox piston through an external pump, allowing controlled variation of the applied pressure. A pressure gauge was used to monitor the system pressure during the test. The hydraulic pump unit used in the experiment and the general test setup are shown in Figure 3-1, while the assembled dropbox under test is shown in Figure 3-2.

Figure 3-1 Hydraulic pump and pressure measurement system used in the experimental study

Figure 3-2 Dropbox assembly under test conditions

At the beginning of the experiment, the system pressure was set to approximately 25 bar, corresponding to a fully disengaged clutch state. The pressure was then gradually reduced in discrete steps of 1 bar. After each pressure reduction, the mechanical state of the dropbox was examined to assess whether torque transmission between the input and output shafts was present.

The assessment of clutch engagement was performed through a functional mechanical inspection. During each pressure step, one operator applied manual torque to the input gear of the dropbox while the output gear was held stationary. As long as the clutch remained disengaged, the input shaft could be rotated freely relative to the output shaft. When the applied pressure dropped below a critical value, resistance to rotation was observed, indicating that the friction discs had come into contact and torque transmission had been re-established through spring preload.

The pressure level corresponding to the onset of torque transmission was identified as the disengagement threshold. A photograph of the pressure gauge at the moment when free rotation of the shaft was no longer possible is presented in Figure 3-3. This pressure value represents the experimentally measured hydraulic pressure required to bypass the spring preload and maintain the clutch in a disengaged state.


Figure 3-3 Pressure gauge reading at the onset of clutch engagement during pressure reduction

The experimentally observed disengagement pressure provides a direct validation point for the analytically calculated hydraulic pressure presented in Section 3.1. The experimental results confirm that the clutch disengagement behaviour occurs within the pressure range predicted by the analytical model, demonstrating consistency between theoretical design calculations and physical system response. A quantitative comparison between analytical and experimental pressure values is presented and discussed in the following section.

### 3.3. Comparison of Analytical and Experimental Results

In this section, the analytically calculated hydraulic disengagement pressure is compared with the experimentally observed pressure required to transition the dropbox from 4×4 to 4×2 operation. The objective of this comparison is to evaluate the consistency of the analytical design model with the physical behaviour of the system under test conditions.

The analytical calculations presented in Chapter 2 and summarized in Section 3.1 indicated that a hydraulic pressure of approximately 11.08 bar is required to overcome the Belleville spring preload and fully disengage the wet multi-disc clutch. This value was obtained based on the piston geometry, total spring preload force, and the effective hydraulic area, assuming ideal force transmission and uniform pressure distribution.

During the experimental study described in Section 3.2, clutch disengagement was observed at a pressure reading close to 11 bar. Due to the analogue nature of the pressure gauge and the gradual pressure reduction procedure, the exact disengagement point could not be identified as a single discrete value. Instead, disengagement was detected within a narrow pressure range around 11 bar, which is consistent with the analytically predicted value.

It should be noted that several factors contribute to the uncertainty associated with the experimental pressure measurement. First, the pressure gauge used in the experiment has a finite accuracy class, which inherently limits the resolution of the reading. Second, the disengagement criterion was based on functional observation of torque transmission rather than direct measurement of axial force or disc separation. Third, variations in oil temperature, internal leakage, and static-to-dynamic friction transition within the clutch pack can influence the precise pressure at which disengagement occurs.

Despite these sources of uncertainty, the close agreement between the analytically calculated disengagement pressure and the experimentally observed value demonstrates the validity of the analytical design approach. The experimental results confirm that the hydraulic pressure required to bypass the spring preload lies within the predicted range and that the clutch disengages reliably without requiring excessive hydraulic input.

Furthermore, the conservative assumptions adopted in the analytical model-particularly in the estimation of spring preload force and drag torque-provide additional confidence in the robustness of the design. The slight deviation between analytical and experimental values is considered acceptable for this type of mechanical–hydraulic system and does not compromise the functional performance of the dropbox.

Overall, the comparison between analytical predictions and experimental observations indicates that the developed design methodology accurately captures the governing physical mechanisms of the wet clutch system. The agreement between theory and experiment validates the selected spring configuration, hydraulic piston sizing, and disengagement strategy for the 4×4 to 4×2 transition.

# 4. CONCLUSION

In this study, the design, analytical verification, and experimental evaluation of a hydraulically actuated wet multi-disc clutch system integrated into a tractor dropbox were presented. The primary objective of the work was to determine the feasibility and reliability of a clutch-based mechanism enabling the transition between 4×4 and 4×2 drive modes under severe operating conditions.

A conservative design approach was adopted by selecting the tractor configuration with the highest torque demand derived from duty cycle data. The required dropbox output torque was calculated based on front wheel power, vehicle speed, and gear ratios, and this torque value was used as the design basis for the wet clutch system. Analytical formulations were employed to determine the required axial clamping force, spring preload characteristics, and hydraulic disengagement pressure.

The Belleville Spring system was designed and verified in accordance with relevant international standards. Stress evaluations confirmed that the operating point remains within the safe and monotonic region of the spring characteristic curve, with maximum stresses remaining below the conservative material strength limits. The selected spring configuration was shown to provide the required preload force while maintaining sufficient safety margins.

The hydraulic piston system was analytically sized to overcome the spring preload and enable clutch disengagement. The required hydraulic pressure was calculated as approximately 11.08 bar, which is compatible with the hydraulic capabilities of the tractor transmission system. In addition, drag torque generated during the disengaged state was evaluated using a conservative continuous film assumption. The calculated drag torque was found to be negligible relative to the maximum engine torque and was therefore not expected to influence system performance.

An experimental study was conducted to validate the analytical predictions regarding clutch disengagement pressure. The experimentally observed disengagement occurred at a pressure level close to the analytically calculated value. Despite inherent measurement uncertainties associated with manual observation and analogue pressure readings, the experimental results demonstrated good agreement with the analytical model.

Overall, the close correspondence between analytical calculations and experimental observations confirms the validity of the proposed design methodology. The results demonstrate that the hydraulically actuated wet clutch system provides a reliable and effective solution for enabling controlled 4×4 to 4×2 transitions in tractor dropbox applications. The methodology presented in this study can be extended to similar drivetrain systems requiring compact, robust, and hydraulically controlled torque transfer mechanisms.

## 5. REFERENCES

[1] H. Renius, Fundamentals of Tractor Design. qwerBerlin–Heidelberg, Germany: Springer, 2020.
[2] British Standards Institution, Disc Springs — Quality Specifications — Dimensions, BS EN 16983:2016. London, UK: BSI, 2016.
[3] British Standards Institution, Disc Springs — Calculation, BS EN 16984:2016. London, UK: BSI, 2016.
[4] European Committee for Standardization (CEN), Cold Rolled Narrow Strip of Steel for Heat Treatment — Part 4: Spring Steels and Other Applications, EN 10132-4:2000 + A1:2002. Brussels, Belgium: CEN, 2002.
[5] Deutsches Institut für Normung (DIN), Heat Treatment of Spring Steels, DIN 17221. Berlin, Germany: DIN.
[6] S. Iqbal, F. Al-Bender, B. Pluymers, and W. Desmet,
"Mathematical model and experimental evaluation of drag torque in disengaged wet clutches," ISRN Tribology, vol. 2013, Art. ID 206539, 2013.
[7] S. Iqbal, F. Al-Bender, B. Pluymers, and W. Desmet,
"Model for predicting drag torque in open multi-disks wet clutches,"
Journal of Fluids Engineering (ASME), vol. 136, no. 2, 2014.
[8] R. G. Budynas and J. K. Nisbett, Shigley's Mechanical Engineering Design, 10th ed.
New York, NY, USA: McGraw-Hill Education, 2014.
[9] M. Bąk, P. Patrosz, P. Śliwiński, P. Załuski, and M. Karpenko,
"Comparison of mathematical models of torque transmitted by multi-disc wet clutch with experimental results,"
in Proceedings of TRANSBALTICA 2022, Lecture Notes in Intelligent Transportation and Infrastructure.
Cham, Switzerland: Springer, 2023, pp. 383–392.